NASA CONTRACTOR REPORT

NASA CR-2
Vol. I of III

NASA CR-2592

RADAR DERIVED SPATIAL STATISTICS OF SUMMER RAIN – EXPERIMENT DESCRIPTION

by

I. Katz, A. Arnold, J. Goldhirsh, T.G. Konrad, W.L. Vann, E.B. Dobson and J.R. Rowland

Prepared by

APPLIED PHYSICS LABORATORY
THE JOHNS HOPKINS UNIVERSITY
Johns Hopkins Road
Laurel, Maryland 20810

for Goddard Space Flight Center

NATIONAL AERONAUTICS AND SPACE ADMINISTRATION • WASHINGTON, D. C. • SEPTEMBER 1975

TECHNICAL REPORT STANDARD TITLE PAGE

1. Report No.	2. Government Accession No.	3. Recipient's Catalog No.
NASA CR 2592		

4. Title and Subtitle	5. Report Date
Radar Derived Spatial Statistics of Summer Rain - Experiment Description, Volume I of III	September 1975
	6. Performing Organization Code

7. Author(s)	8. Performing Organization Report No.
I. Katz, A. Arnold, J. Goldhirsh, T. Konrad, W. Vann, E. Dobson, J. Rowland	

9. Performing Organization Name and Address	10. Work Unit No.
Applied Physics Laboratory The Johns Hopkins University Johns Hopkins Road Laurel, Maryland 20810	11. Contract or Grant No. NASA/DOD Agreement S-70248AG

12. Sponsoring Agency Name and Address	13. Type of Report and Period Covered
National Aeronautics & Space Administration Washington, D.C. 20546	Contractor Report
	14. Sponsoring Agency Code

15. Supplementary Notes

16. Abstract

An experiment was performed at Wallops Island, Virginia, to obtain a statistical description of summer rainstorms. Its purpose was to obtain information needed for design of earth and space communications systems in which precipitation in the earth's atmosphere scatters or attenuates the radio signal. Rainstorms were monitored with the high resolution SPANDAR radar and the 3-dimensional structures of the storms were recorded on digital tape. Volume I of this series describes the equipment, the experiment and tabulates all data obtained during the experiment.

Volume II contains a description of the analytical techniques used and the resulting statistical description of rainstorms. Volume III is a collection of some of the more important technical notes issued during the program.

17. Key Words (Selected by Author(s))	18. Distribution Statement
Precipitation, radar, radar-weather, space communications, scatter, attenuation, rain cell statistics	Unclassified - Unlimited Cat 47

19. Security Classif. (of this report)	20. Security Classif. (of this page)	21. No. of Pages	22. Price*
UNCLASSIFIED	UNCLASSIFIED	98	$4.75

For sale by the National Technical Information Service, Springfield, Virginia 22161

EXECUTIVE SUMMARY

INTRODUCTION

Earth and earth-space communications links are affected by precipitation along the transmission path. Terminals set up to take advantage of space diversity must be spaced in a manner dependent on rain intensities, rain cell sizes, and spacings. Unwanted interference also occurs because of scattering from the precipitation particles. Communications engineers urgently need statistical information on rain shower intensities and their geometrical properties.

A NASA sponsored experiment was carried out at Wallops Island, Virginia in 1973 to provide such data. One of the S-band radars, the Space Range Radar (SPANDAR), was modified to meet the needs of a radar specifically aimed at studying precipitation processes.

This report, Volume I, describes the radar changes, the rain cell statistics program, and the data collected. In Volume II are found details of the data reduction and analysis program. Volume III contains some of the more important memoranda issued during the course of the experiment.

SYSTEM DESCRIPTION

Radar

SPANDAR is a high-power, narrow-beam radar originally designed for long-range tracking. Fine resolution is achieved by the 60 ft antenna (0.4 deg) and the 1 μsec pulse length. Great care was taken with pre-experiment radar measurements and calibrations during the experiment to reduce the combined radar and processing errors to less than 2 dB.

There were changes in the original radar configuration occasioned by the specific needs of the rain cell experiment. These modifications were: frequency diversity capability, digital integration, computer control of the antenna mount, extended linear range of the receiver, and digital and analog video recording providing on-line as well as off-line data processing capability. As a consequence of these modifications the radar can be considered to approach the ideal radar for the radar meteorologist.

Frequency Diversity

It is well known that since meteorological targets fluctuate from pulse to pulse it is necessary to average a number of statistically

independent pulses to achieve a reliable measure of reflectivity. The largest number of pulses averaged is generally limited by scanning considerations while the shortest meaningful time between pulses to be averaged depends on their time-to-independence. For typical weather targets at S-band the time-to-independence is about 20 msec.

Shifting the r-f frequency from pulse to pulse is an excellent way to obtain independence in a short time. With the 1 μsec pulse it was necessary to jump in frequency at least 1 MHz for say 20 successive pulses before returning to the original frequency. The actual frequency shift was in an interlace mode where the frequency interval between pulses was 12 MHz. The interlace pattern was selected to minimize second-time-around weather targets; such interference can be a problem when the rain is heavy. For a 12 MHz frequency jump the second-time-around targets fall well outside the receiver bandwidth.

To accomplish the goal of providing statistical information on rain cells one needs a three-dimensional snapshot of the cell structure. This can be achieved by making a raster scan through the cell before the cell changes. A scan rate of 3 deg per sec was considered sufficiently fast to do this. This rate is adequate if one requires one sample reflectivity per beamwidth and every successive pulse is independent of its predecessor. It can be seen that the appropriate scan rate is a compromise between scanning fast enough to see the entire cell structure before it changes and slow enough to ensure accuracy of measurement; frequency diversity allowed sampling and averaging 128 pulses for 1 sample in each beamwidth.

Digital Integrator

An 871 bin digital integrator capable of integrating 128 to 1024 video pulses was added to the system. It is true that for a stationary process one obtains a more accurate measure of reflectivity the larger the number of pulses in the average. However, adding more samples after about 50 yields an increase in accuracy only very slowly. The specific number of 128 pulses in the average was arrived at for practical reasons.

Computer Control of Antenna

In contrast with most of the previous research performed with the Wallops radars, where manual operation was adequate, this experiment required that antenna scan sequences be executed with little loss of time between sweeps. A PDP-8 computer was interfaced with the antenna mount to perform sequences rapidly and automatically. Stored programs for various scan sequences can be called up quickly via teletype control

resulting in more-or-less stationary rain cell snapshots. Complete three-dimensional snapshots of cell structures were scanned within a four-minute interval; this included azimuthal sectors up to 60 deg in width.

Extended Dynamic Range Log Amplifiers

For this experiment it was deemed important to measure weak rain areas as well as the heavy showers. Calculations for SPANDAR showed that in order to measure a 1 mm per hr rain at the longest ranges, 140 km, as well as heavy thunderstorms at close ranges, 10 km, it would require a receiver linear over a 90 dB dynamic range. This assumed 10 dB pulse-to-pulse fluctuations of the received weather signal. A new solid state log IF amplifier was designed and added to the system to extend its linearity over this range.

Digital and Analog Video Recording

An on-line recording system was made part of SPANDAR for the rain cell experiment. The output of the video integrator was digitized and recorded on a 9-channel, 1600 bits per in. synchronous tape recorder operating at 45 in. per sec. In addition to the integrated output from each resolution cell, the digital tape stored time, antenna mount position, processing parameters as well as all pertinent radar parameters including pulse-to-pulse calibration signals.

An off-line system also was incorporated into SPANDAR as a precaution against loss of data. The basis of this system was an Ampex FR-910 video tape recorder. It is a four-head, spiral-scan recorder to record radar video on a frequency-modulated subcarrier with an input signal bandwidth of 6.5 MHz. Two audio channels are available for recording voice annotation and/or multiplexed data ancillary to the video signals.

Radar video was recorded on the FR-910 and integrated video on the digital tapes. If any malfunction occurred in the processor the original radar video was replayed later through the processor to simulate real-time recording. In fact, the original video tapes still exist and can be replayed at any time for other purposes. The video tapes can also be played back through RHI and PPI scopes using the ancillary data by using the special interface equipment designed for this purpose.

EXPERIMENT DESCRIPTION

The experiment was carried out in two parts. The first part, during the fall of 1972, was essentially a check-out period for the

equipment and procedures, but some useful data were obtained. During the summer of 1973 the full-scale experiment took place using all the equipment as described here.

The general purpose of the experiment was to determine the statistics of intense rain cells using radar. In particular, the objectives were to (1) determine the statistics of the field of rain cells in terms of such descriptors as cell size, intensity, spacing, number density, and altitude dependence; and (2) find the detailed structure of individual cells leading to a model of an individual cell for use by communications scientists and meteorologists.

For the first objective the operational mode was to take a set of PPI scans, usually over 360 deg, at a 2 deg elevation angle at one-half hour intervals. For the cell model objective a mode of operation was used involving rapidly-taken PPI raster scans. In this mode a 60 deg sector was selected and one, or a series of, raster scans were made to examine the three-dimensional structure and its changes with time.

The preliminary experiment ran from 15 September to 6 October 1972. The full-scale experiment covered the period 9 May to 31 August 1973.

METEOROLOGICAL CONSIDERATIONS

As is apparent in any radar-weather experiment certain synoptic mesoscale and perhaps microscale weather data are needed. One must forecast precipitation in order to carry out the experiment economically. One needs point rainfall measurements and other meteorological observations to help relate the radar measurements to the broader meteorological situation and also to help in extrapolating the rain cell statistics to other climatic regions.

The Weather Service at Wallops Island was used as the primary source of weather information. Surface observations and radiosonde data were made available along with all the teletype and facsimile charts from the networks. In addition, weather briefings were held each morning which included local forecasts. A tipping bucket rain gage was installed about 12 mi north of SPANDAR especially for this experiment; this was augmented by rainfall data at Wallops, Patuxent, Dulles, Atlantic City, and Richmond.

ACCURACY AND CALIBRATION

Considerable effort was placed on measuring the radar system carefully. The antenna gain is now known precisely, system stability

was checked by frequent calibrations. The overall SPANDAR accuracy may be stated to be within 1.7 dB standard deviation.

DATA SUMMARY

In the 1972 experiment there were 10 rain days and 123, 360 deg PPI scans at one-half hour intervals and 35 PPI raster scans were obtained to study individual cells in three dimensions. In the 1973 experiment there were 33 rain days with 96 one-half hourly PPI scans and 403 PPI raster scans. A total of 1141 discrete rain cells were processed from these data.

Fortunately for this experiment, the 1973 summer period had more rain and more days of rain than the preceding 10-yr average primarily because May and August exceeded the averages by a substantial amount.

Page Intentionally Left Blank

VOLUME 1--EXPERIMENT DESCRIPTION

CONTENTS

CONTENTS (Continued)

CONTENTS (Continued)

Page Intentionally Left Blank

ILLUSTRATIONS

ILLUSTRATIONS (Continued)

TABLES

1. INTRODUCTION

Ground stations transmitting to communications satellites will under certain propagation conditions suffer atmospheric attenuation and may also interfere with beyond-the-horizon ground communications links operating on the same frequencies. Because of severe spectrum limitations and a consequent intense interest in frequencies above 10 GHz, it has become necessary to obtain propagation and interference information on which one can base decisions in communications systems design. One must either limit transmitted power or assure adequate separation of the stations. In either case, decisions must be based on quantitative interference measurements or accurate predictions based on such measurements.

There are various mechanisms for propagating short electromagnetic waves beyond the horizon. For the radio frequencies being discussed here, the important causes of scatter are ducts, layers characterized by high variance in refractive index, and discrete scatters such as aircraft, birds, and precipitation. Crane (Ref. 1) has concluded that precipitation scatter is the most important of these mechanisms for the communication interference problem.

In that same paper he also concluded that the statistics of the small, strongly reflecting rain cells were unavailable. Such cells are difficult to describe statistically because of their infrequent occurrence. Ground-based measurements obtained with rain gages are inadequate for this purpose because of the small likelihood of a cell passing over a gage. Only a large network of closely spaced gages can be used to study such cells, for example Semplak and Keller (Ref. 2).

The most appropriate tool for observing such phenomena is high resolution radar. Large areas ($\sim 4 \times 10^4$ km^2) can be observed frequently (within minutes) and with high resolution ($\sim .4$ km). Statistics such as the distribution of cell sizes and intensities, typical cell separation, frequency of occurrence and cell lifetimes are but a few of the important characteristics measurable with radar. A reasonable approach is to determine the above statistics using radar and relate them to local rain gage measurements and a characterization of the rain type. It is likely that these relationships can ultimately be inverted to predict the expected statistics of rain in other areas using only local surface rainfall data.

The objective of this experiment was to collect radar data which could yield such statistics on the spatial distribution of summer rain cells. Ideally one would like simultaneous, fine-scale measurements in both time and space over a large volume, i.e., over a 200 km

radius and all altitudes to 15 km. In practice, however, this ideal set of data cannot be realized using only a single radar for a variety of practical reasons. For example, because of the long time-to-independence of meteorological scatterers and the number of independent radar samples on target needed to provide a good statistical estimate of reflectivity, the time to probe such a large volume with a 0.5° beam is much longer than the fine time scale needed to establish cell lifetimes. This incompatibility leads to the definition of two well defined objectives, each of which is capable of being handled by a radar. These objectives, then, defined particular modes of operation for the radar system in the presently described experiment.

The first objective concerned the determination of the statistics of the field of rain cells, i.e., sizes, and spacings, the so-called cell field mode. The second objective was to determine the detailed structure of individual rain cells leading to the description of a cell model. In this case, relationships such as reflectivity as a function of altitude, size (both vertical and horizontal) and time development were needed. This mode of operation involved probing selected rain cells at a fine time scale and with fine spatial resolution.

The experiment was carried out in two phases. The first occurred during September and October 1972 and emphasized testing and calibrating the equipment. The second phase was the full-scale data collection period providing the statistical base of one summer season, May through August 1973.

Background for this experiment is contained in Refs. 3 through 8. These technical notes contain the details of the equipment, the experimental procedures and the original data analysis plan for obtaining the statistics of the time-and-space distribution of rain.

This final report is divided into three parts. Volume I contains a description of the radar and associated equipment and the modifications made to carry out the experiment, certain meteorological considerations and a summary of the data collected during the experiment. The data reduction, analysis techniques and results are presented in Volume II. Some of the more important Technical Notes are reproduced in Volume III. Also, since this experiment was so multi-faceted, it was deemed advisable to prepare a cross-index to aid in finding source material in the Technical Notes; this cross-index will be found in Section 8 of this volume.

2. SYSTEM DESCRIPTION

2.1 SPANDAR

The Applied Physics Laboratory of The Johns Hopkins University has been operating a Radar Atmospheric Research Facility (RARF) at Wallops Island continuously since 1965. Support for the program came jointly from the Air Force and NASA. The radar facility is owned by NASA, Wallops Island and is part of their comprehensive radar, rocket and weather facilities. To date, RARF has been used in a variety of research problems associated with clear-air atmospheric processes as well as with precipitation.

The Space Range Radar (SPANDAR) is the S-band radar system used for the rain statistics problem being discussed here. It is a precision, long-range, conical scan, tracking radar used primarily for the collection of deep space trajectory data and secondarily for range safety, orbit determination, and vehicle performance analysis. Its special features include a pulse doppler tracking subsystem and a digital range subsystem that yields unambiguous range data to 250,000 nmi.

The SPANDAR facility is located on the mainland, about 2 mi west of Wallops Island. The facility building houses transmitters, receiver, ranging equipment, data handling equipment, recording equipment, and a complete test and repair shop. Adjacent to the building is the antenna tower housing the receiver, rf-head equipment, parametric amplifiers, encoders, antenna drive components, and antenna pedestal.

The technical characteristics of SPANDAR are shown in Table 2.1. Note that two transmitter tubes are available.

One transmitter tube was designed by Raytheon and is unique. Replacement parts must be built as needed so that cost of repair and replacement is fairly expensive. The other is from an FPS-18 radar. FPS-18 radars are used extensively so that replacement parts are available in quantity at low cost. In addition, maintenance procedures are well established. Peak power output of the FPS-18 transmitter is 1.2 MW as opposed to the 5 MW from the Raytheon tube. Since high power is not necessary for the purpose of studying rain, the FPS-18 was considered adequate and was used throughout the experiment described here.

The receiver system includes a parametric amplifier with approximately a 20 dB gain. Saturation with the paramp operating is

Table 2.1

SPANDAR Configuration Characteristics

Transmitter Subsystem	
Frequency range	2,700 to 2,900 MHz
Peak power output	Raytheon Transmitter 5 MW FPS-18 Transmitter 1.2 MW
Pulse width	1, 2 or 5 μsec
Pulse repetition rate (PRF)	160, 320 or 640 pps
Receiver Subsystem	
Frequency range	2,700 to 2,900 MHz
Type	Superheterodyne
Dynamic range	70 dB (modified to 90 dB)
Noise figure	2.5 dB
Sensitivity	-117 dBm for 240 KHz bandwidth
I.F. frequency	30 MHz
Low noise device	Parametric amplifier
Bandwidth	Matched to pulse width
Antenna Subsystem	
Reflector	60 ft parabola
Feed	Nutating
Polarization modes	Circular, vertical or horizontal
Scan	Conical
Gain	52.8 dB
Beamwidth	0.39° (half power points)
Beam cross over	1.5 dB
Azimuth coverage	360° continuous
Elevation coverage	0 to 90°
Tracking rates	5° sec^{-1}
Angle slewing rates	12° sec^{-1} azimuth; 17° sec^{-1} elevation

around -50 dBm so that when the paramp is removed from the line, a saturation level of -30 dBm is reached.

The mixer-preamplifier is located in the building at SPANDAR and the output of the paramp, which is located on the antenna feed, is brought down by cable. Higher level signals may be observed when the paramp is out by placing attenuators in the line prior to the mixer. The dynamic range of the log IF system was 70 dB, modified to 90 dB for this experiment, with a minimum detectable signal of -117 dBm with the paramp in the system. The SPANDAR antenna is a 60 ft diameter paraboloid having a pencil beam whose width is 0.4 deg; its gain is 52.8 dB. A photograph of the antenna reflector is shown in Figure 2.1. It is capable of continuous azimuthal rotation at angular speeds up to 12 deg sec^{-1} in azimuth and 17 deg sec^{-1} in elevation. In elevation the antenna provides coverage up to 90 deg.

There were changes in the original SPANDAR configuration occasioned by the specific needs of the spatial statistics experiment. These modifications were:

a. Pulse-to-pulse frequency diversity into the FPS-18 transmitter (Ref. 10)

b. Computer control of the 60 ft antenna pedestal for various scan schemes

c. Log amplifiers added to extend the dynamic range of the receiver

d. Integration of 128 pulses with digitization into 871 range bins

e. Computer control of the data acquisition and formatting for processing, detection and analysis on an IBM 360/95 computer

f. Digital and analog data recording on magnetic tape

g. Pulse-to-pulse calibration of the radar video output

h. Analog magnetic tape playback through the radar receiver and digital data acquisition system.

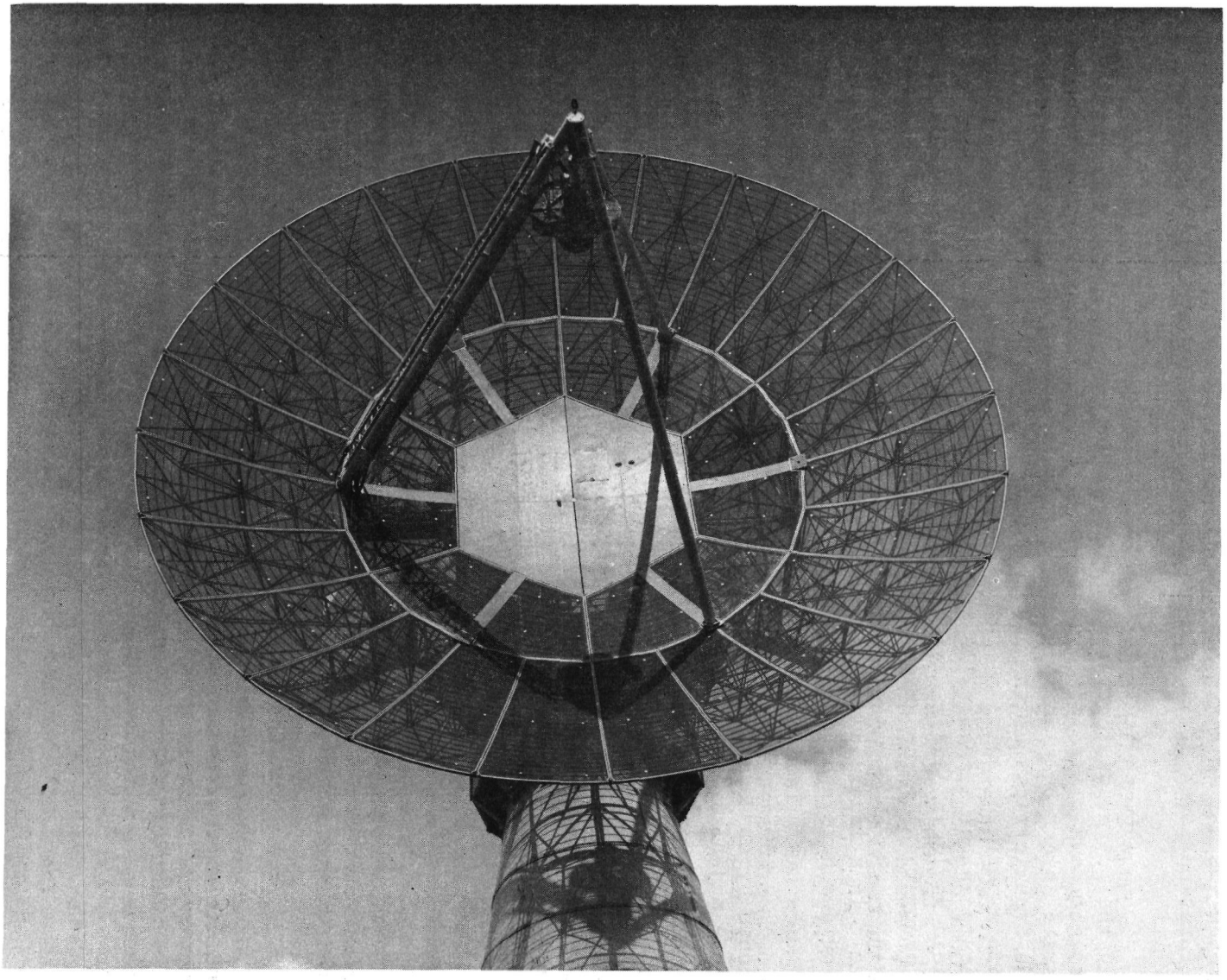

Figure 2.1. SPANDAR Dish and Feed

Details of these modifications may be found in Refs. 9, 10, 11, 12, 13 and 14.

2.2 FREQUENCY DIVERSITY

Radar returns from meteorological targets fluctuate from pulse to pulse so that it is necessary to average many pulses to achieve a reliable measure of reflectivity. The pulses to be averaged must be statistically independent. A more detailed discussion of this point is contained in Section 3.3 on measurement accuracy. The greatest number of pulses averaged is generally limited by scanning considerations whereas the shortest meaningful time between pulses to be averaged depends on the time-to-independence, i.e., the decorrelation time. The time to independence, τ_s, for typical meteorological scatters observed at S-band is about 10 to 30 ms (Atlas, Ref. 15 and Marshall and Hitschfeld, Ref. 16). Samples taken at intervals less than τ_s do not contribute significantly to the accuracy of the result although some benefit is gained by averaging partially correlated samples. The turbulence associated with thunderstorms would result in τ_s being near the lower end of the above range.

One practical method for achieving independent samples more quickly than τ_s is by the use of frequency diversity (FD). Wallace (Ref. 17) shows that independence can be achieved by pulse-to-pulse frequency shifting. The correlation coefficient ρ between two echoes $\Delta\nu$ apart in frequency is given by:

$$\rho = \left[\frac{\sin\pi\tau\Delta\nu}{\pi\tau\Delta\nu}\right]^2$$

where τ is the transmitted pulse width. Thus, complete decorrelation or independence from one pulse to the next is achieved if each pulse is shifted in frequency by $1/\tau$.

If no decorrelation technique is used such as frequency, spatial, or aspect diversity, an inordinately long time is required to accumulate enough independent pulses to calculate an accurate mean radar reflectivity. Frequency diversity (FD) capability was added to the SPANDAR radar for this purpose. A 1 μs pulse length was used so that the frequency had to be shifted by at least 1 MHz for 20 successive pulses or more before returning to the same frequency.

The FPS-18 transmitter, used in this program, has a usable bandwidth of 30 MHz. There are two frequency stepping modes. In the first mode the frequency is stepped in 1 MHz increments as described

above for 24 steps. The second is an interlace mode where the frequency interval between pulses is 12-13 MHz. This second logic, Figure 2.2, was included to minimize the second-time-around problem, i.e., the detection of targets within the second (and even third) ambiguous range interval. The latter logic was used extensively through the 1973 experiment.

The FD equipment consists of a solid state (tunnel diode) microwave oscillator unit controlled by digital frequency stepping logic, see Appendix A, Volume III or Ref. 14. The output of this oscillator is up-converted to the desired transmit and local oscillator frequencies by modulating the basic oscillator frequency (f_o) with lower frequencies (240 MHz and 270 MHz) which are separated by the radar IF. Additional circuits included in the FD chassis to provide a calibrated reference signal are a time-delayed and pulsed sample of the transmit signal and a pulsed noise source. These two signals are combined in a microwave network and made available to the radar receiver in a common line. A block diagram of the FD unit is shown in Figure 2.3.

The pulse delay and frequency-stepping logic generator unit is comprised of delay multivibrators, presettable counters, an adder and gates to provide the delayed pulses to the pulse modulator and noise diode source and frequency step circuit. The frequency step circuit accepts the delayed input trigger and steps the output frequency 8, 16, 24 or 32 times before resetting to the starting frequency. A mode control switch is provided to select fixed frequency, linear steps (ramp) or an interlace mode where an adder is enabled and disabled on alternate pulses to separate adjacent transmitted frequencies by the 12-13 MHz discussed previously. The digital-to-analog converter and the shaping circuit convert the output of the digital frequency selector unit to an analog voltage, adjusts the gain for 1, 2, or 4 MHz per step and shapes the output voltage so that each digital step results in the same oscillator frequency shift.

2.3 RADAR VIDEO PROCESSOR AND CONTROLLER

Because of the requirement to obtain three-dimensional "snapshots" of storm cells it was necessary to perform many of the data gathering and processing functions automatically. A PDP-8I computer was installed to direct the antenna for the rapid scan sequences. Stored programs allowed the operator to select particular scan sequences for rapid execution.

A digital integrator, also under the direction of the PDP-8I, integrated 128 video samples in each of the 871 range gates and recorded these data on IBM-compatible tapes. A photograph of the processing and

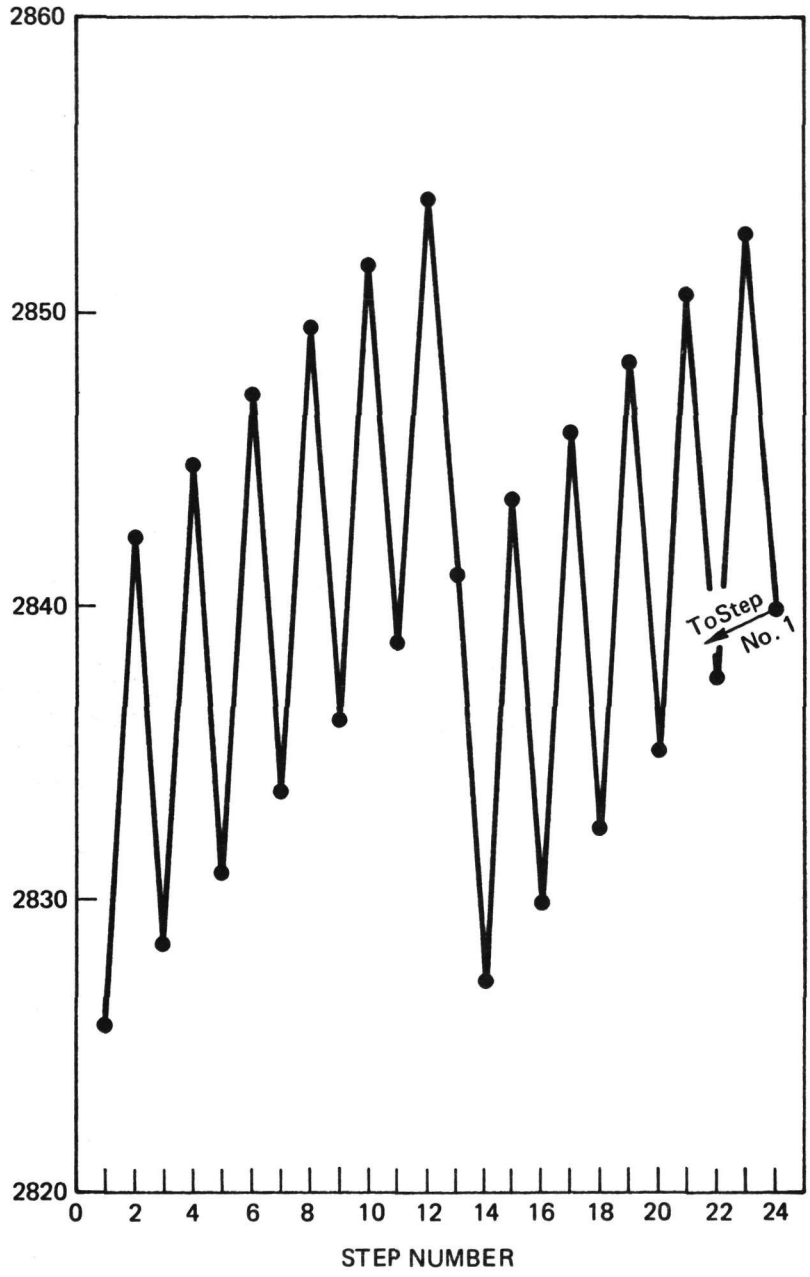

Figure 2.2. Frequency Diversity Stepping Logic

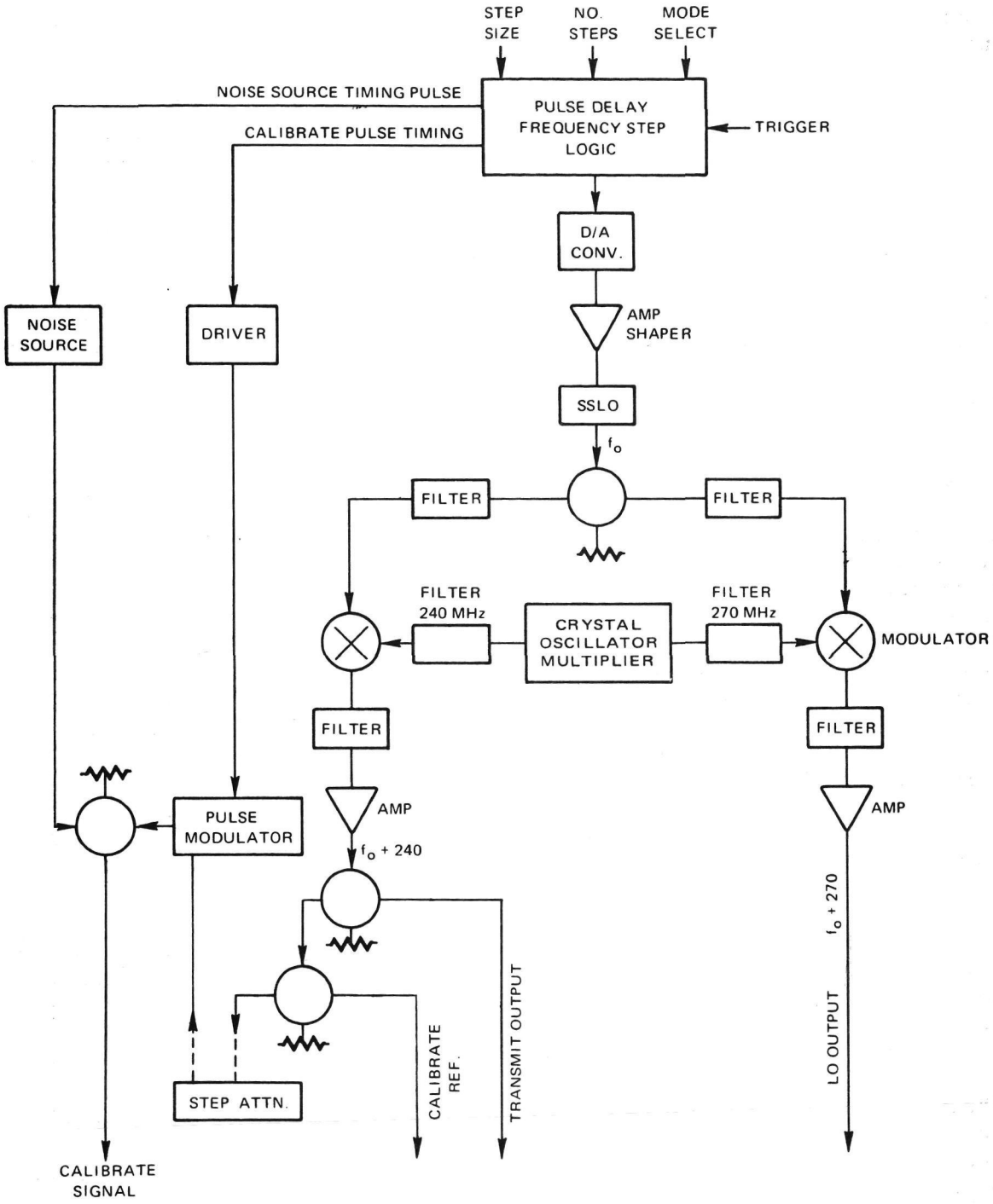

Figure 2.3. Block Diagram of Frequency Diversity Unit

controlling equipment, the tape recorders and the teletype for input information is shown in Figure 2.4.

A description of the control and processing equipment in terms of the method of processing on-line and off-line follows.

2.3.1 On-Line Processing

The on-line system performs four distinct functions: it digitizes and integrates the radar signal in each of the spatial resolution cells, records the integrated video on digital magnetic tape and provides antenna scan commands in real-time. The elements of this system shown in Figure 2.5 include the radar video processor (RVP), digital tape recorders, the PDP-8I computer, the radar control and the RVP-Control Interface units, Refs. 18, 19, 20, 21.

The function of the RVP is to sample the incoming radar signal in each spatial resolution cell, digitize these data and integrate for the required number of pulses. To provide a reasonably accurate estimate of the reflectivity, the signal in each resolution cell must be averaged. A minimum of 128 pulses in the average was chosen which gives a statistical error of less than 0.4 dB, 80 percent of the time. The number of pulses integrated was chosen based on considerations of prf, antenna scan rate and accuracy of the reflectivity estimate. A prf of 960 sec^{-1} and 128 pulses in the average was used and the antenna scan rate was 3 deg sec^{-1}.

The spatial resolution in the radial (range) direction is one pulse length (1 μs which corresponds to 150 m). The RVP accommodated 871 range cells to cover the desired range increment from 10 to 140 km. The output for each cell is the mean log power received (log A^2) in the form of an 8 bit word which is recorded on the digital tape recorder in IBM compatible format. Major features of the RVP are shown in Table 2.2.

The digital tapes are 9 channel, 1600 bpi, synchronous machines which operate at 45 ips. Two tape transports are used with a controller for continuous operation. No time or data are lost due to changing tape reels. In addition to the integrated output from each resolution cell, the digital tape also stores time, the mount positions, processing parameters as well as all pertinent radar parameters including calibration signals. Timing signals are provided to the RVP by the RVP-Control Interface. This interface also conditions the data from the radar to the RVP. The control of the RVP and digital tapes is provided by the PDP-8I computer.

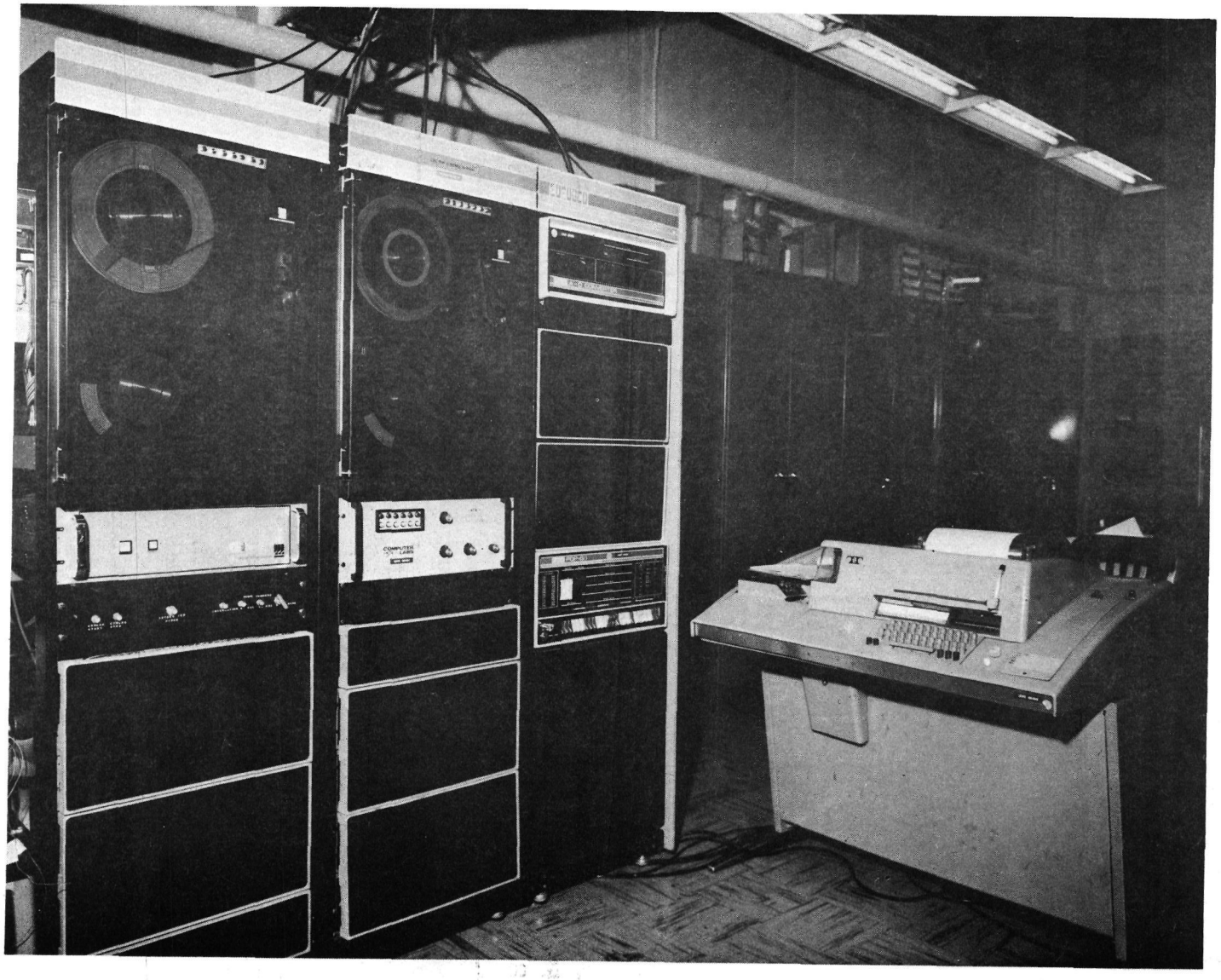

Figure 2.4. Radar Video Processing Equipment Showing Digital Tape Recorders and Teletype Input

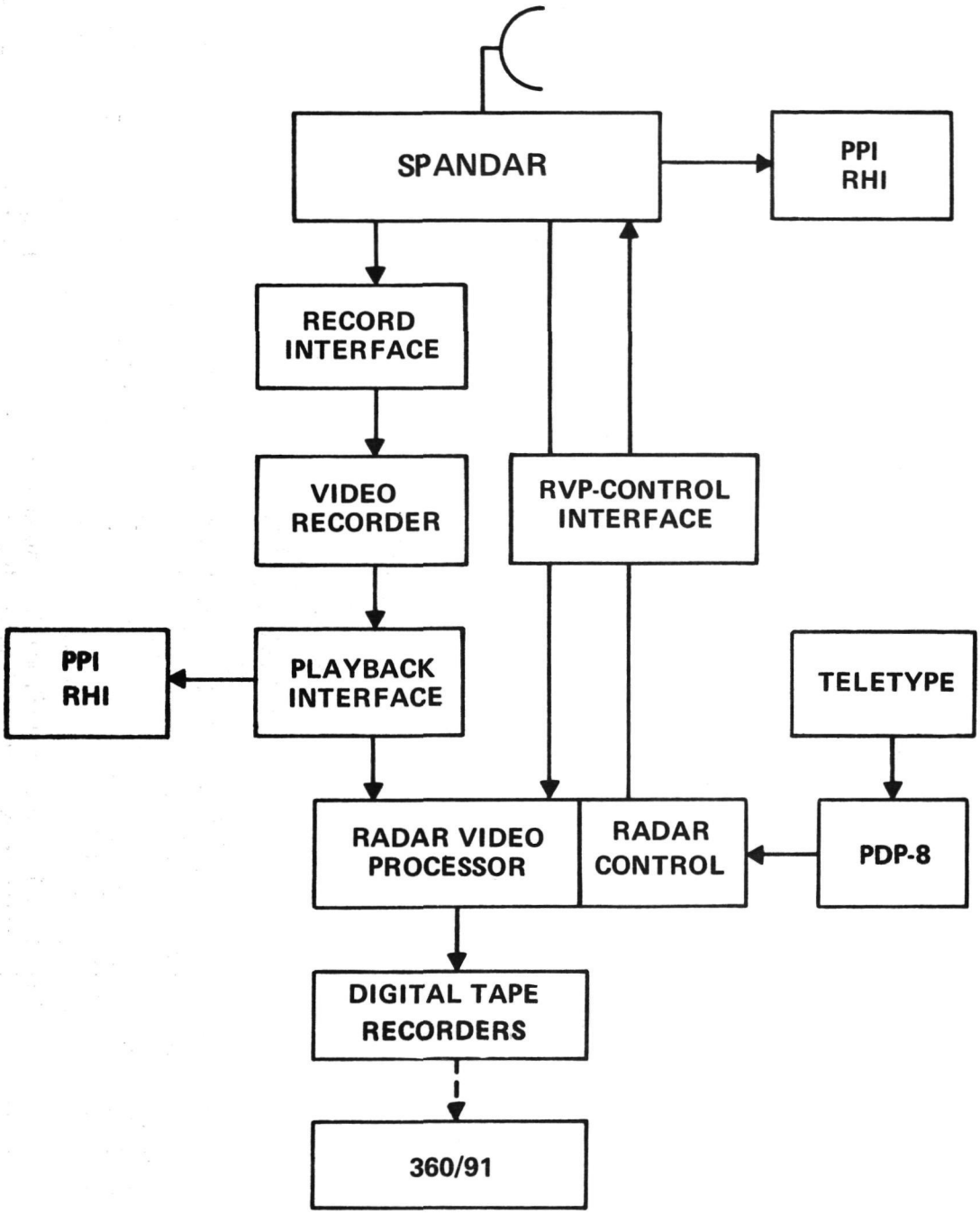

Figure 2.5. Block Diagram of Radar Control Processing and Recording

Table 2.2

Major Features of the Radar Video Processor

RADAR VIDEO PROCESSOR
871 Range Cells - 10 to 140 km
Digitize Video, Integrate 128 Pulses
Antenna Scan Rate 3 deg sec^{-1}
Sample Video at 4 MHz Rate
Output: 8-bit Word on Magnetic Tape
MAGNETIC-DIGITAL TAPE
9-Channel, 1600 BPI, 45 in. per sec
Synchronous, IBM-Compatible
Two Tape Transports for Continuous Operation
Stores: Video, Time, Azimuth, and Elevation
Processing Parameters
Radar Parameters

The PDP-8I computer also controls the antenna mount through the Radar Control and the RVP-Control Interface. Programs are stored in the computer which command the mount to execute prescribed scanning sequences such as 360 deg scans, Range Height Indicators (RHI) or Plan Position Indicators (PPI), raster scans, etc. Selection of scan parameters such as azimuth start, stop, range segment to be recorded, execute commands, etc., are operator input to the computer via teletype. The computer also contains internal self checks which ensure proper operation.

2.3.2 Off-Line Processing

Whenever any element in the on-line data acquisition system was inoperable (the digital tapes and transports and that portion of the RVP-Control Interface which controls the RVP), the off-line system was used. This system consists of an Ampex FR-910 video tape recorder and two interface units, Refs. 22 and 23. The tape recorder is a studio-type video recorder modified for instrumentation use. It is a four-head, spiral-scan recorder which records the video radar signals on a frequency-modulated subcarrier with an input signal bandwidth of 6.5 MHz. Special amplitude and phase-balancing controls are provided to allow precise alignment of the signals to the four heads and eliminate switching transients. Two audio channels are also available for recording voice annotation and/or multiplexed data ancillary to the video signals.

The record interface provided buffering of the incoming video signals to match the recorder's $\pm$ 1.0 v input voltage and to mix the prf sync trigger on this video channel. Coded time (NASA format), bearing and elevation shaft encoder signals and other pertinent header (digi-switch entry) information was recorded as a multiplexed pulse train on one audio channel. The 960 prf is counted down to provide the shaft encoder strobe signal and the frame sync gate for each frame of the multiplexed input data.

The playback interface had two functions. It allowed data to be played into an RHI or a PPI scope for inspection and it provided proper inputs for the RVP. Thus the interface unit had the capability of separating the prf sync pulse and the video signals and to restore the video to the original input levels. The transfer gain through the recorder was kept at unity. Major features of these two interface units are shown in Table 2.3.

The digital data on the audio track is decoded for playback and analysis with selectable front panel light display, sin/cos outputs operate scope displays and a computer function organizes all the data

Table 2.3

Major Features of Interface Units

INTERFACE - RECORD

- Buffer to Match FR 910 ± 1.0 v Input
- Mix PRF Sync Trigger on Video Channel
- Coded Time (NASA Format) } On Audio
- Azimuth & Elevation Shaft Encoder Signals } Channel

INTERFACE - PLAYBACK

- Playback Video Tapes into RHI & PPI
- Separate Sync Pulse From Video
- Playback thru RVP
- Digital Data on Audio, Decode for Analysis
- Display on Front Panel Lights
- Sin/Cos Operate Scopes
- Computer Function to Give 8 or 9 Bit Words for PDP-8I

into 8 or 9-bit words suitable for processing by the PDP-8I computer (an integral part of the RVP equipment) for recording on a 9 bit IBM 360 compatible tape. The sin/cos azimuth and elevation signals with 14 bit resolution is outputted on each frame at 150 v for smoothed scope operation.

The RVP equipment whose functions have been described above also had appropriate software written to enable SPANDAR to be operated automatically. This permitted the scanning to be made with great economy of time. A detailed description of the processor and controller, constructed by Computer Science Corporation, can be found in Appendix B and Ref. 21.

2.4 DISPLAYS

2.4.1 SPANDAR

Real-time displays of the radar returns were available at SPANDAR. They enabled the investigators to monitor the weather situation, to identify and designate the rainfall areas to be recorded and to serve as a guide in later analysis to check cell locations, intensity, area covered, etc. Two sets each of Polaroid photographs of the PPI and RHI were taken for all sweeps. Examples of PPI and RHI photographs taken during the experiment are shown in Figures 2.6 and 2.7. In addition, two other scopes were available for the 35 mm camera for backup photographs. A photograph of the bank of RHI and PPI scopes is shown in Figure 2.8. Log video and sliced (grey scale) video presentations were used. Log video showed all rain areas, including the lightest rain. Sliced video was used to obtain a quantitative measure of the rain intensity and aided in the selection of the more appropriate rain areas for studying the individual cells.

2.4.2 WSR-57 Facsimile Recorder

The Weather Service of NOAA operates a WSR-57 weather radar at the Patuxent River Naval Air Station on the Chesapeake Bay approximately 90 km N.W. of Wallops Island, Virginia. This radar is part of the weather radar network of the Weather Service and is used for weather depiction over the Washington, D.C. area.

The WSR-57 information in the form of a PPI display, is presently sent to the Weather Service Station at Wallops Island via a leased telephone line and displayed on a WBRR-68 Facsimile Recorder. Normally the WBRR-68 transmitter is configured to show a 238 km display. This range is quite sufficient to cover the area of interest at Wallops, the 140 km radius circle, and to provide adequate forewarning of approaching weather systems. However, 603 km can be displayed and transmitted

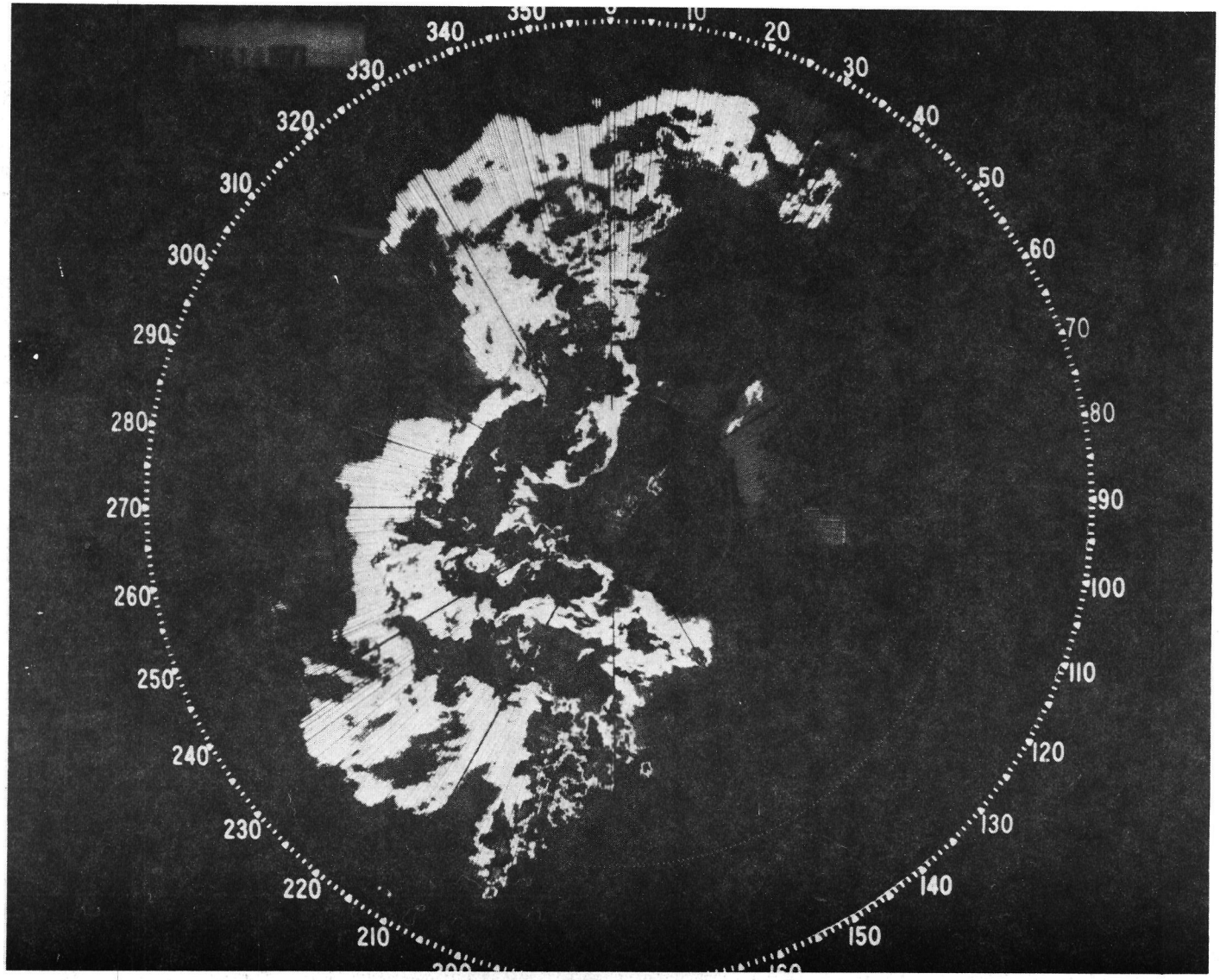

Figure 2.6. Example of PPI Photograph During Rain Experiment

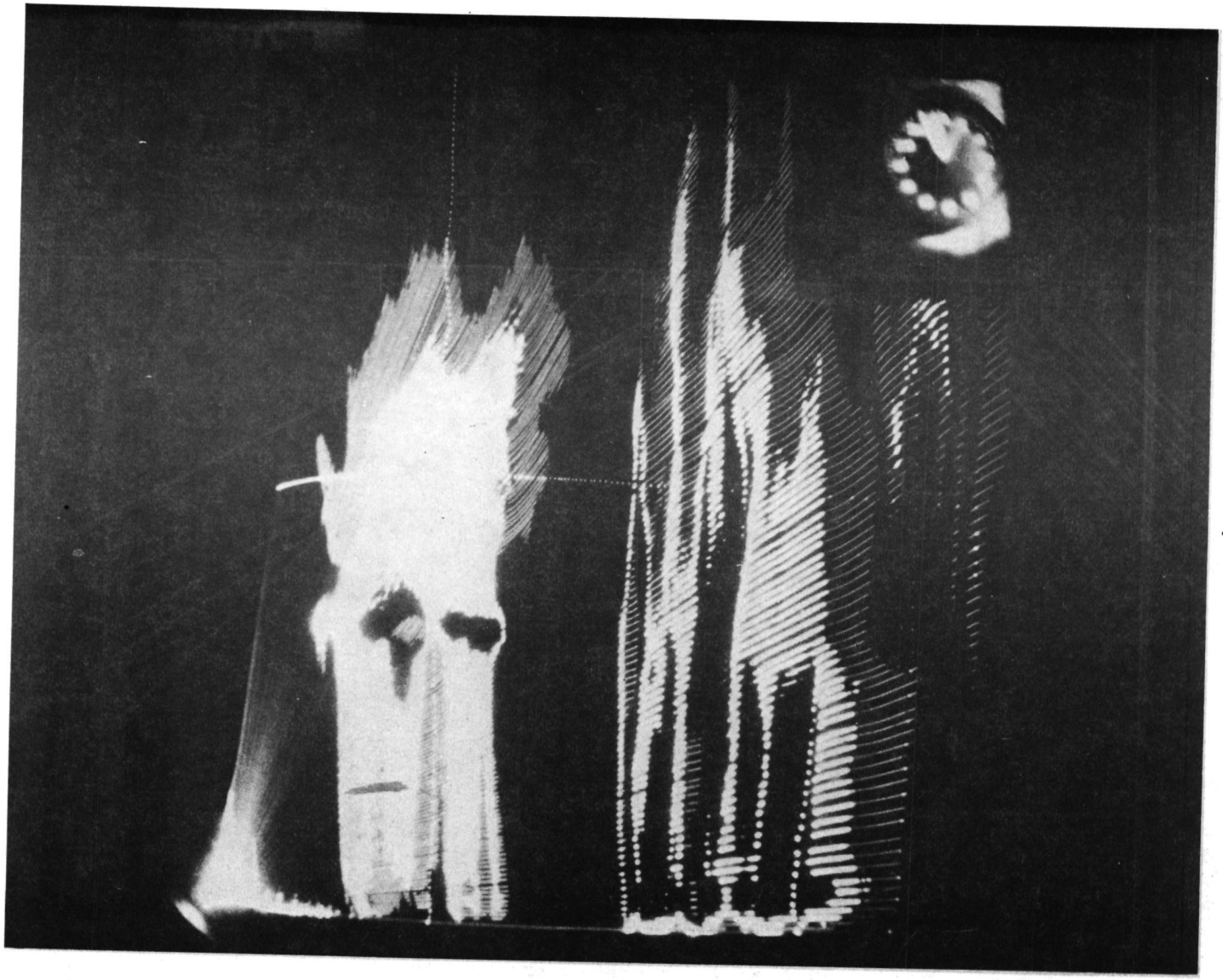

Figure 2.7. Example of RHI Photograph During Rain Experiment

Figure 2.8. Bank of RHIs and PPIs Scopes at SPANDAR

on request. Figure 2.9 shows the overlapping coverage of the two areas of observation.

One hundred seconds are required to produce a picture on the WBRR-68 transmitter. This fixes the highest picture rate at once every 2 min. A variety of other display rates are available, e.g., once every 5 min, 10 min, 1 hr, etc. A high quality land line was made available from NASA Main Base to SPANDAR. A facsimile recorder was located at SPANDAR for use primarily as a forecasting tool.

A video integrator and processor (VIP) designed specifically to interface with the WSR-57 (not to be confused with the video processor designed for SPANDAR) is used at the Patuxent River and other Weather Service stations. The VIP is used to provide a contoured display of the radar returns which correspond to specified rain intensities. The resolution element is fairly large, 1.85 km (1 nmi) in range and 2 deg in azimuth. A three rpm antenna slew rate is normally used. The range displayed when signal contouring is used is from 18.5 km to 230 km. Log video is used with the VIP to provide 53 dB of dynamic range. Range correction is included. The contour display is 3 shade, 2 cycle, yielding six levels of rain intensity up to 10 in. per hr.

The integrated and contoured data provided a gross check against the quantitative data taken at SPANDAR. In addition, the intensity contour display showed the most intense storms prior to their entering the 140 km radius of observation and provided forewarning of approaching storm systems.

3. EXPERIMENT DESCRIPTION

The first phase of the experiment was carried out during the fall of 1972 in which all equipment available at that time was tested. Some data were collected during this phase. The full-scale experiment was performed during the summer of 1973 with all of the equipment operating as described in this report.

This section discusses the experiments, operational procedures, calibration techniques and accuracies, theoretical and measured (Refs. 10, 11, 13, 24, 25, 26, 27, 28, 29, 30, 31, 32 and 33).

3.1 1972 EXPERIMENT

The preliminary experiment was carried out from 15 September to 6 October 1972. Since the Radar Video Processor and Controller were

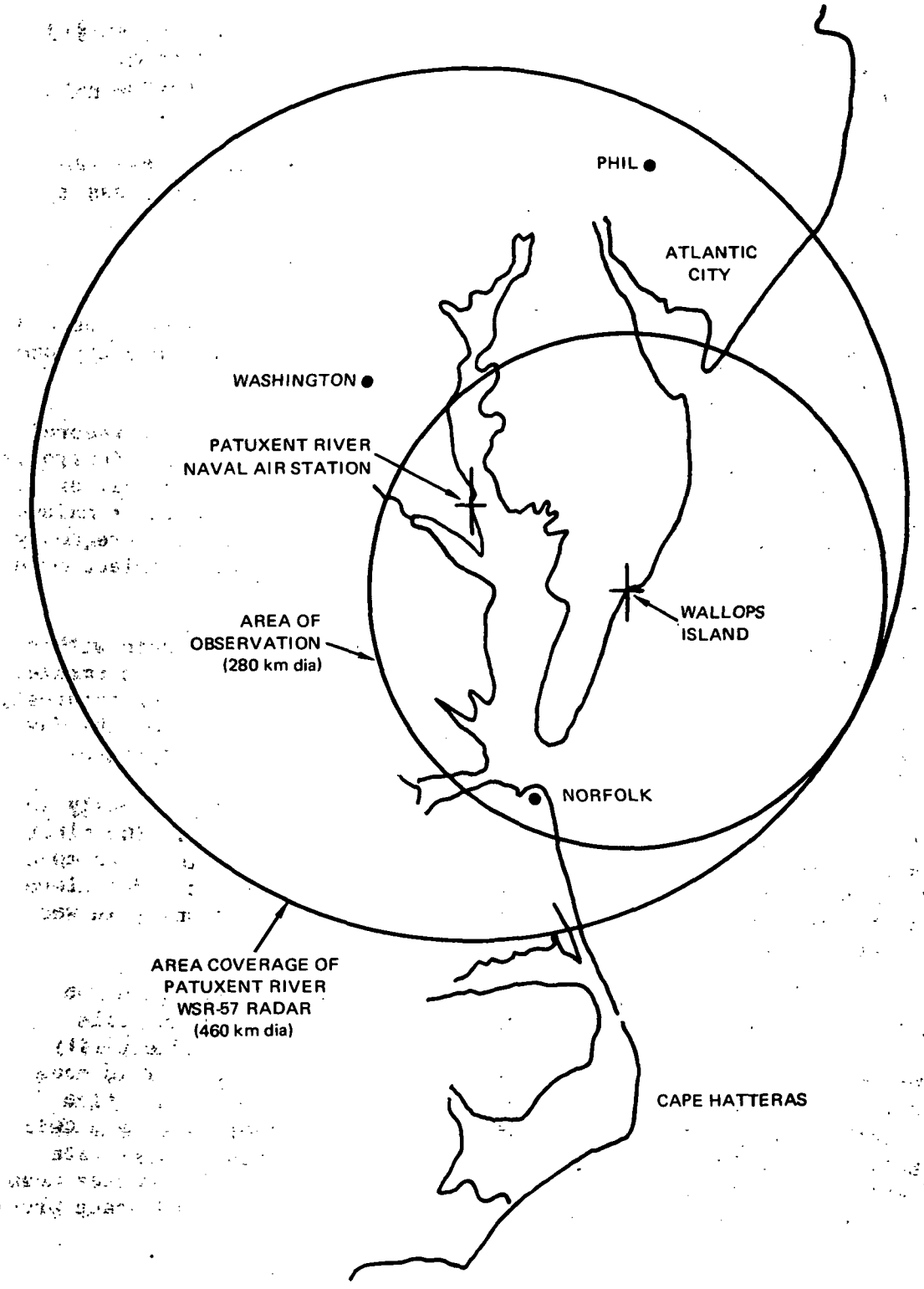

Figure 2.9. SPANDAR and PATUXENT WSR-57 Radar Coverage Operation

not yet available at that time all storms were recorded on the FR-910 video tape recorder described in Section 2 and on Polaroid film. Frequency diversity components were operating but with a 24-step sequential logic and not with the logic shown in Figure 2.2.

Data taken during this period were obtained while the radar was under manual control. Data obtained in this mode were processed "off-line" as described in Section 2.3.1.

3.2 1973 EXPERIMENT

The 1973 Summer Experiment took place in the period between 9 May and 31 August 1973. This was the full-scale experiment and the one which yielded the data analyzed and reported in Volume II.

From the start of the summer experiment until 29 May recording was on video tape. On that date the Radar Video Processor and Controller became operational and the experiment went into computer control, or into the "on-line" processing mode. The processor and control remained in operation and has now become an integral part of SPANDAR. Frequency diversity for the entire Summer of 1973 was operated in interlace mode as shown in Figure 2.2.

It was not economically feasible to record every rain within the 140 km range of the radar. The philosophy was to collect a smaller number but still representative sample of the summer storms of interest. The observation times in terms of the number of days, hours of the day and frequency of observations were chosen to reflect this approach.

Two modes of operation were used, as mentioned previously in Section 1, each consistent with the two primary objectives. The first objective was to obtain a description of the field of cells. Its mode was a set of PPI scans, usually covering 360 deg, taken at 2 deg elevation at one-half hour intervals throughout the time when any rain was detectable by the radar within the 140 km range.

The second objective of this program was to determine the detailed spatial and temporal characteristics of single rain cells leading to a statistical cell model. In this case, the reflectivity structure as a function of altitude and time was measured. This mode of operation involved rapidly probing selected rain cells on a fine time scale and with fine spatial resolution. For example, once a cell or group of cells was selected the radar probed in stepped elevation PPI series through the cell or cells. This is called a PPI raster scan. The single-cell mode, then, concentrated fine scale time and space probing

in a prescribed, limited volume. This mode was interlaced between the statistical mode observations.

A full description of the operations plan will be found in Reference 13. However, to make this experiment description more meaningful selected sections of the operations plan which guided the procedure in obtaining data are reproduced in Sections 3.2.1 through 3.2.3.

3.2.1 Equipment Setup

"A. SPANDAR will be used to collect data from the 1973 summer experiment. The FPS-18 transmitter with frequency diversity and no paramplifier will be used throughout. Pulse length will be 1 μsec. Antenna slew rate will be set at 3 deg sec^{-1}.

B. The prime data recording will be on digital magnetic tape. This equipment, called the RVP, digitizes the incoming video signals, integrates 128 pulses for each of the 871 range gates and records the average on the DigiData 1600 bits-per-inch magnetic tape. There are two tape transports and data are recorded on each sequentially; when one tape is completed the other is activated automatically so no data are lost.

C. The video tape recorder, FR-910, will be in use all summer as a backup recording system. At the start of the experiment all data will be recorded on the FR-910. This requirement may be relaxed after some of the digital tapes are processed through the IBM 360 computer and all equipment is found to be operating satisfactorily.

D. An interface system has been designed to allow us to operate:

a. SPANDAR with FR-910

b. SPANDAR with RVP

c. FR-910 with RVP

d. FR-910 with scopes.

E. Displays and Recording Techniques. Displays of the storm cells must be available in real time to facilitate decisions in the day-to-day operations. The following displays will be available:

a. Facsimile recorder display of the Patuxent River WSR-57 radar operating during the experiment, this is called PAXFAX.

b. There will be two PPI and one RHI scopes with photographic recordings.

c. The video slicer equipment will be installed at SPANDAR to provide quantitative estimates of storm cell intensities. Six slice levels will be used. Slice settings will vary depending on the rain intensity at the time. Recording will be on Polaroid and 35 mm film."

3.2.2 Daily Operations: Radar

"The sequence of events to be followed is (see Ref. 13):

1. Activate the radar system, scopes, FR-910, RVP interfaces, Fax recorder, slicers, photographic and other recording equipment.

2. Set up RVP and FR-910.

3. After warm up period calibrate radar, processors and recording equipments by stepped attenuation method.

4. Scan PAXFAX output for indication of rain activity.

5. Now follow flow diagram shown in Figure 3.1. Techniques involving scan modes and calibrations on tape will be found in Refs. 8, 11, 20 and 21.

6. After a storm abates the operation will revert to the watch mode on PAXFAX and SPANDAR.

7. Full calibrations will end each day's operations. This will include replaying of video tapes to test the presence and adequacy of data on tape. Checks of Digitapes and RVP operation should also be made.

8. The interface has controls which must be set before each scan. These are required to provide data identification of equipment status and experiment parameters. These will include:

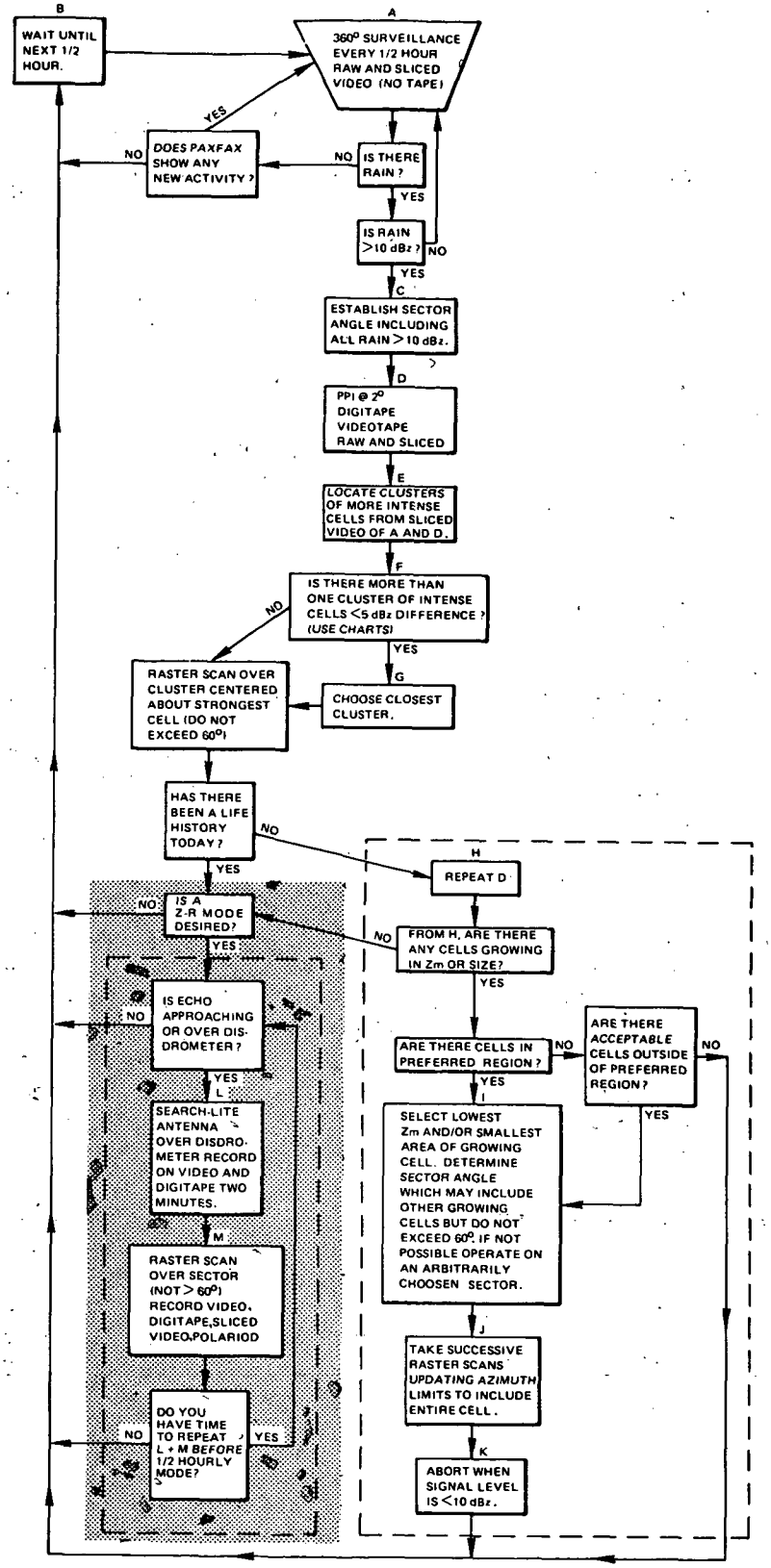

Figure 3.1. Operation Flow Chart for Rain Statistics Experiment

a. Year, day, sweep number

b. Time (this is set in automatically)

c. Azimuth and elevation limits

d. Angle change for successive scan in a raster scan mode

e. Type of run: RHI or PPI

f. Number of scans in a sequence

g. Radar status: prf, pulse width, scan rate, data validity

h. Calibration levels

9. A detailed written operations log will be kept to record the sequence of events during a daily experiment. These logs will include all the information a. through h. above as well as supplementary information as equipment malfunction, if any. Standard RHI and PPI logs will be kept for Polaroid and 35 mm photographs. The FR-910 also has an audio channel on which data a. through h. above should be voice-recorded.

10. Data handling will require care since there will be so much of it and in such a variety. Video tapes will always be documented and kept at the SPANDAR site since it requires the FR-910 for playback. Digitapes will be transferred SAP to APL for processing. Polaroid photographs, logs, weather data, strip chart records, calibrations and weather notes will be documented and returned to the RAP project at APL once per week.

11. The SPANDAR operation, starting May 7, 1973, will be on a 3:00 p.m. to 11:30 p.m. shift. Four operators will be assigned to that shift on a rotation basis. The Site Manager (SM) will be on a shift which is split between the rain and the clear air research. The Project Director (PD) will start his daily shift with the 2:00 p.m. weather briefing."

3.2.3 Graphical Aids

"A. Figure 3.2 is a height-range chart for various antenna elevation angles. Range is in nmi out to 100 and height extends up to 70,000 ft. The chart was drawn for a 4/3 earth radius.

B. Radar power vs reflectivity factor. This chart is Figure 3.3. On the upper chart we have radar power received, dBm plotted against reflectivity factor, dBZ for selected values of distance from 10 to 140 km. Note these are for nominal values of τ and k. On the lower chart we have rain rate vs reflectivity factor for selected Z vs R relationships. Ordinates are given in mm hr^{-1} and in hr^{-1}.

C. Figure 3.4 is included to aid in normalizing power values for the various ranges. Power received in dBm at 1 nmi is plotted against range in nmi for various values of radar received power over the range of interest for this summer's experiment. A -30 dBm signal at 10 nmi for example, is found on this graph to be -50 dBm (normalized to 1 mi); this corresponds to a -13 dBm signal at 70 mi.

D. Figure 3.5 is plotted to give a quick look at the change in elevation angle required to give an approximate change in vertical height of 1 km and 2 km. These are approximate because the angle change for a given height change is different at different altitudes at the same slant range."

Note that the flow diagram, Figure 3.1, contains a Z-R mode of operation. Although efforts were made to use a disdrometer and a rain gage along with the radar to obtain a Z-R relationship for various rainstorm intensities, the disdrometer under loan from another organization, did not operate satisfactorily. That portion of the flow diagram which is shaded was not used in any significant way; therefore it may be considered "inoperative" for this experiment.

3.2.4 Meteorological Instrumentation

Two different types of meteorological data were required in support of this experimental program. One set of data concerned the mesoscale and synoptic features of the weather system and the other set of data the point measurement of the rainfall. In the former case, the

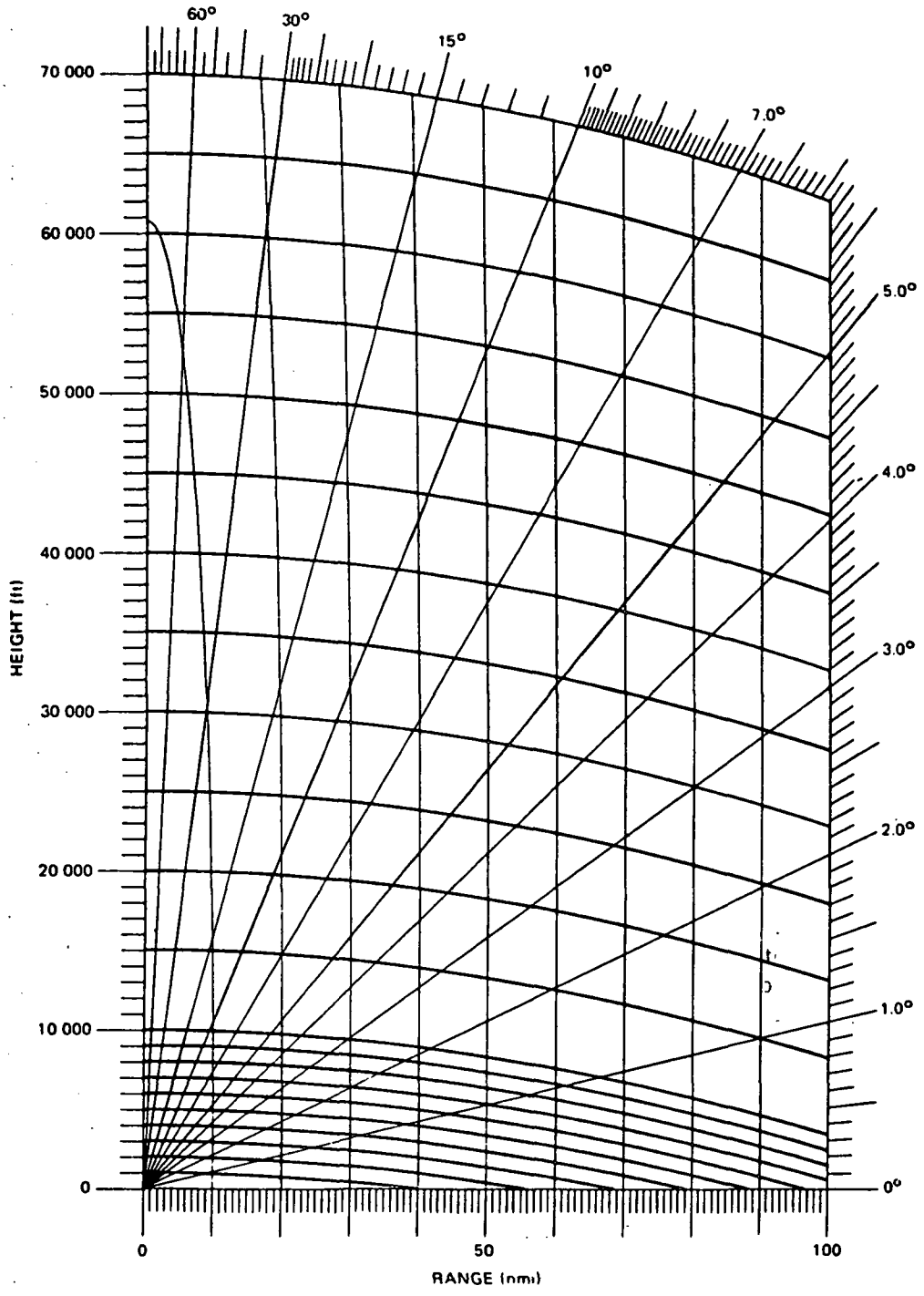

Figure 3.2. Height Range Chart for Various Elevation Angles

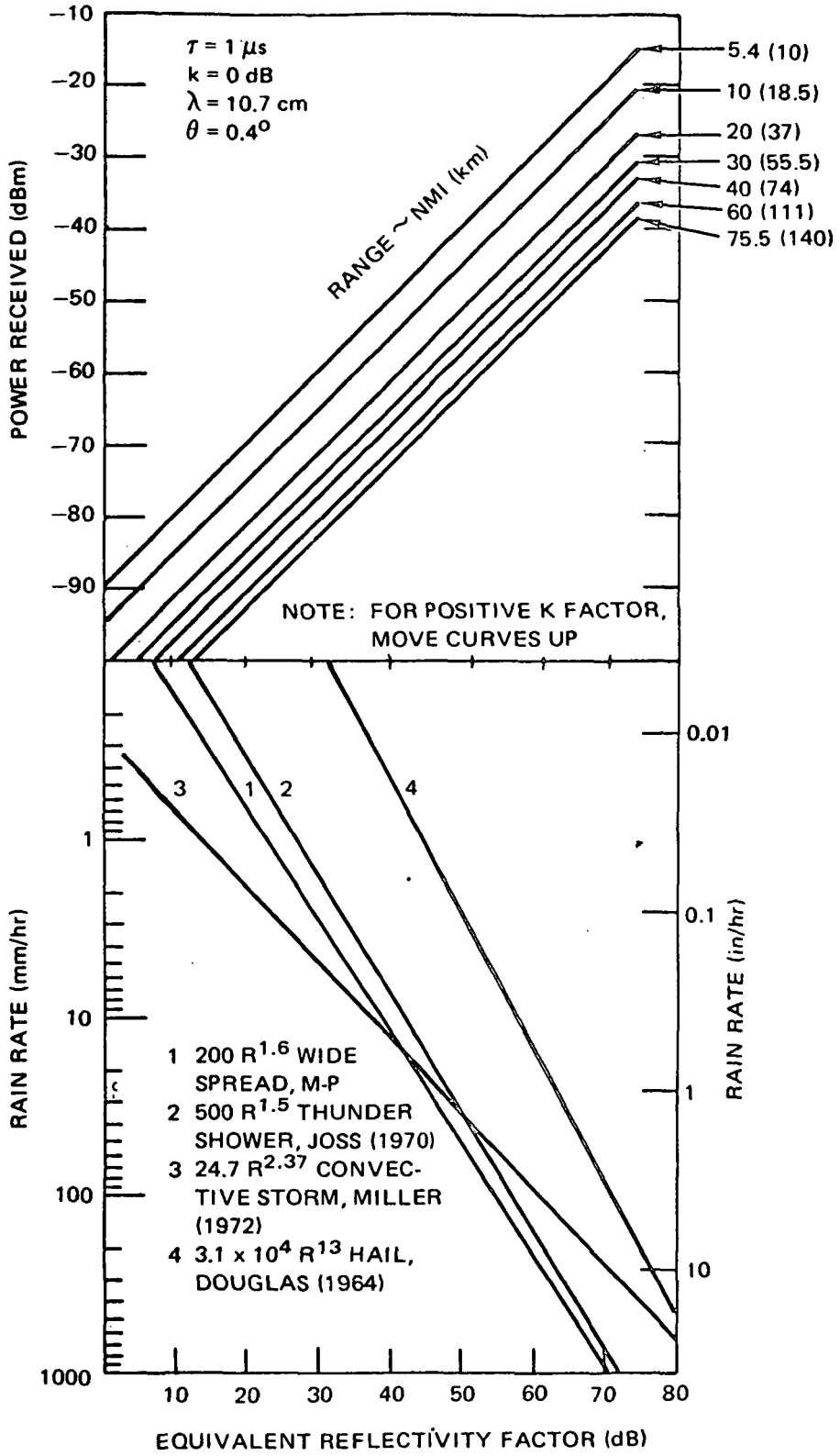

Figure 3.3. Radar Power Versus Reflectivity Factor for Various Ranges (upper chart); Rain-Rate Versus Reflectivity Factor for Various Z-R Relationships (lower chart)

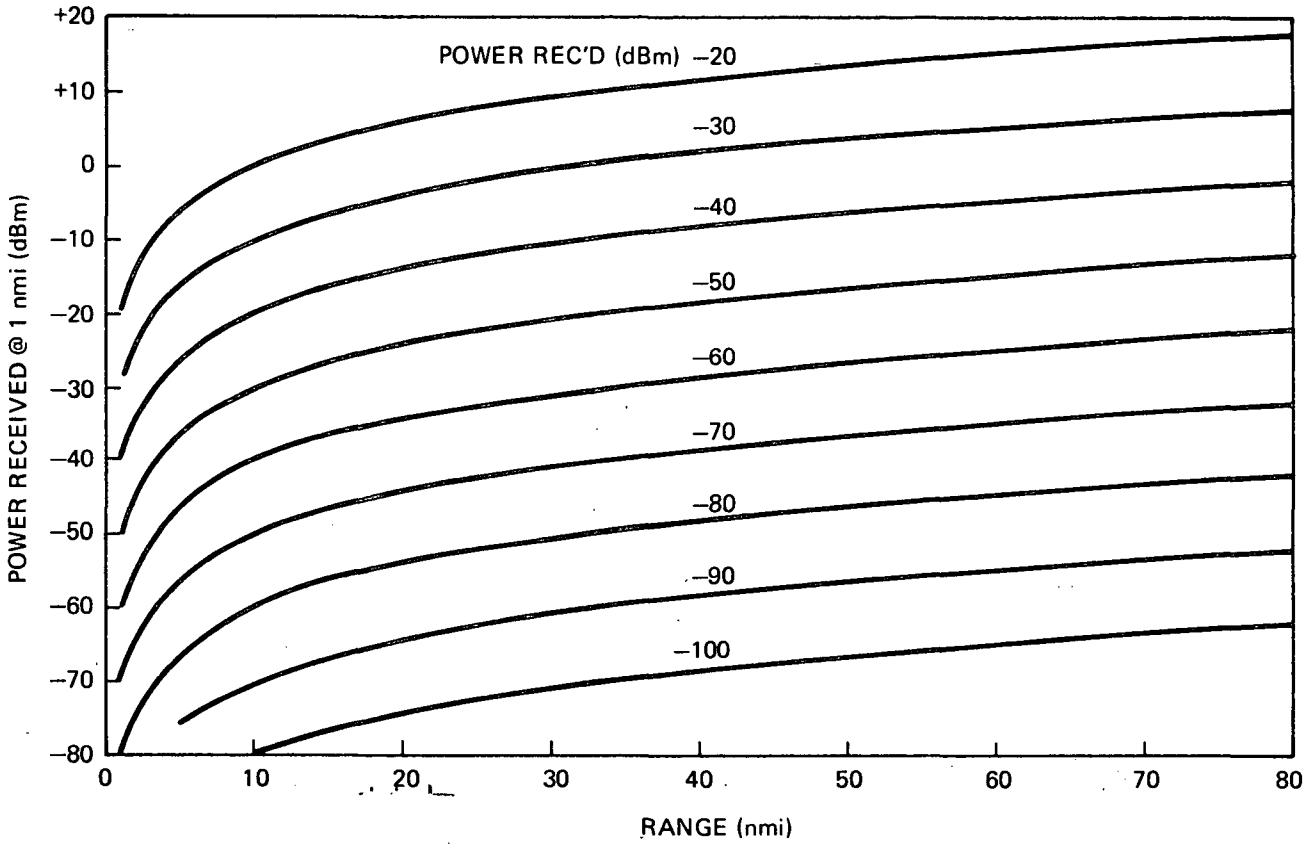

Figure 3.4. Range Normalization Curves for Various Power Levels

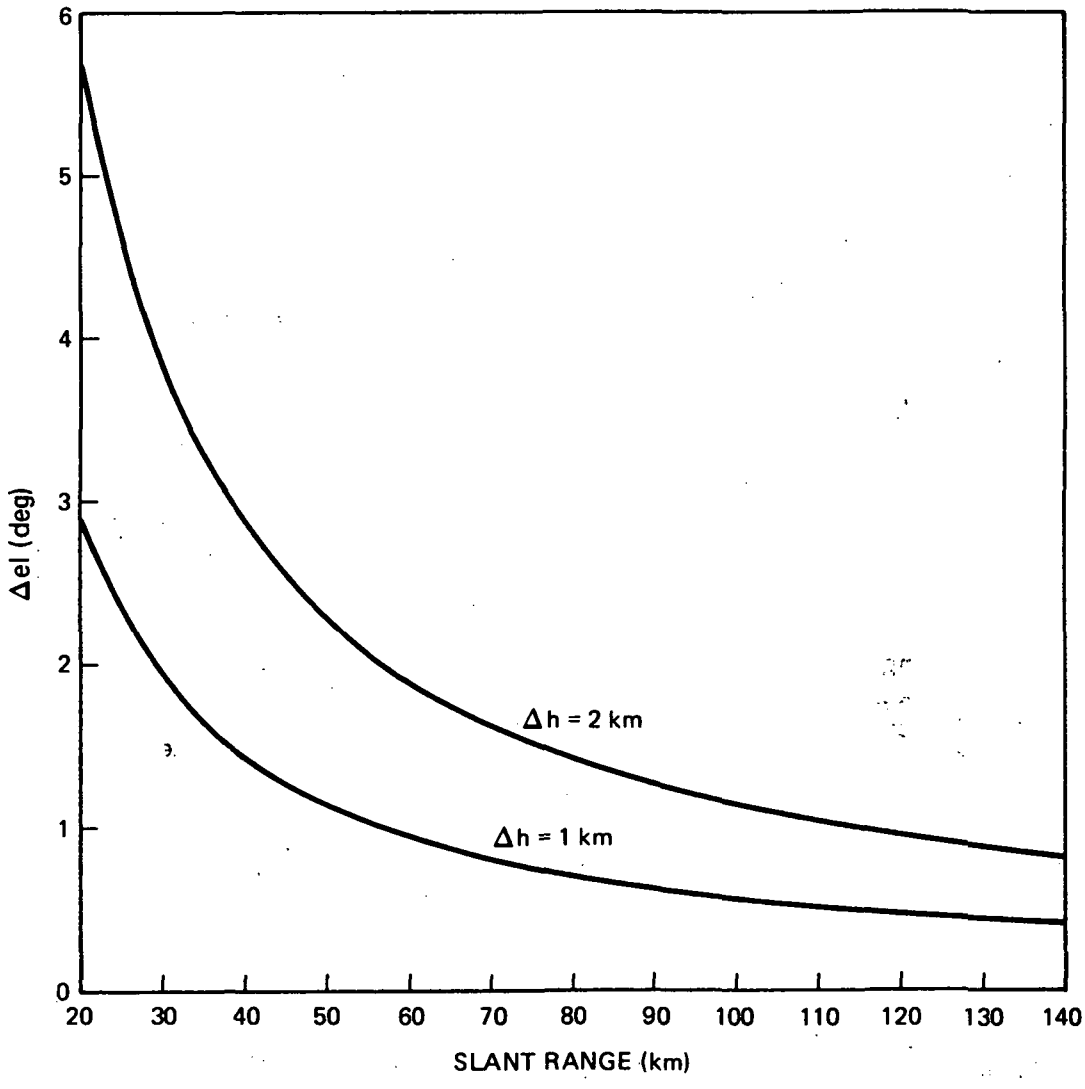

Figure 3.5. Elevation Angle Change to Produce A Change in Altitude As A Function of Range

facilities for collecting and recording the data were in existence and available at Wallops Island and other Weather Service stations in the area. In the latter case, the instrumentation was installed and operated by APL personnel. Since the two sets of data serve entirely different purposes they will be discussed separately.

Mesoscale and synoptic weather data were required for three reasons: (1) for the purpose of forecasting; (2) for the purpose of relating the radar data and the point rain measurements to the broad meteorological development; and (3) for use in categorizing the rain types and in extrapolating the results to other regions.

The Weather Service station at Wallops was used as the primary source of weather information. Surface observations, radiosonde data and surface measurements were made available along with all the facsimile charts from the Weather Service network. In addition, weather briefings were held each morning which included local forecasts.

Surface observations and radiosonde data from other Weather Service stations such as Washington, Hatteras and Greensboro were also assembled. The radar data from the Weather Service radar at Patuxent River was available at the Wallops Island Weather Service station and at SPANDAR.

3.2.5 Point Measurements

The radar-rain relationship, commonly referred to as the Z-R relation, is needed to translate the radar reflectivity (Z) measurements within the storm cells into rain rate (R) and total water content (M). Rain rate alone, as determined from ground-based rain gages such as tipping buckets, is not sufficient. Joss et. al, Ref. 34, has found good agreement when the drop size distribution, rain rate and radar reflectivity were categorized in terms of the type or rain, i.e., drizzle, widespread and thundershower. Categorization is needed if extrapolation to other areas is to be attempted.

Point rainfall measurements were made and were an integral part of the operation. A tipping bucket rain gage was installed at the VOR site, about 12 mi north of the radar site. These data are augmented by rainfall data from other existing weather stations, i.e., Wallops Station, Patuxent, Dulles, Atlantic City and Richmond. As part of the experiment plan specific instructions were issued to the Project Director related to the meteorological requirements. Some of these instructions are quoted below.

3.2.6 Daily Operations: Meteorological

"A typical sequence of events involving the PD and meteorological aspects of this experiment is as follows:

"1. The PD visits the forecaster on duty at about 1400, before start of the 1500 shift. The PD obtains information on whether rain/showers are expected within 140 km of SPANDAR for the period 1500 to 2330, and, if so, from what direction it is expected to first appear. If forecaster states the type of rain expected, this should be recorded on the metlog. Also, the forecaster should be asked if he expects cirriform clouds (but not anvil cirrus), and his answer is recorded. If it is already raining at 1415, or has been raining, find the likelihood of another rain period before 2300 EST. This information is desired for guidance to the PD and need not be recorded.

2. The PD will use the information transmitted by the Patuxent radar to our site. The transmitted copies of PAXFAX should be retained for archiving. If date or time is not clearly legible, the PD should enter these on the copy. Note: The Patuxent radar information is advisory. We may be in better position than Patuxent to observe rain first appearing from the South to East. There may be convective situations in which showers develop spontaneously in our observation region so there is no early warning from the Patuxent radar.

3. When we are actually observing rains or showers with SPANDAR, the PD informs the Weather Service that we are observing precipitation. This is needed because this initiates a special set of information from them, required for our analyses.

4. The PD (possibly requiring assistance of site personnel) has the responsibility for maintenance of the rain gage. He visits the gage to change charts, check tipping bucket operation, general operation of the gage measurement and other checks described below."

"a. Chart change. Prior to removal of old chart he jogs pen, to show record termination, and writes date and time (EST) on the chart. Correspondingly on new chart, pen jog denotes record start; date and time

(EST) are entered on chart. Chart is moved to correspond to the correct time, allowing for backlash. The box containing the chart record is marked with location, "rain gage," date and time of beginning and end of record and rain amount (see below). While a chart will easily record for one week it is desired that the chart be changed during a non-rain period, or if unavoidable (say, near end of chart) during a light rain since we want to avoid loss of any rain tip information. It is desired to obtain rain gage records through the period of the summer experiment, whether or not there are radar observations.

b. Miscellaneous. The inking of the charts are verified from examining the end of the old chart. Fresh inks are added to pens as necessary. Pens are replaced and ink flow checked as necessary. Determine, if possible, if there has been a power interruption, and, if so, if the time of power outage is known or can be estimated. A note containing this information should be included in the metlog. The tipping bucket is tipped manually 10 times at the end of the chart record. If the chart does not show 10 tips, attempt to repair or report problem. If there is water in the tipping bucket, estimate if it is less than half full in which case it is neglected or more than half full in which case note at the end of the chart that there is a residual .01 in. rain. However, the manual tipping of the bucket is not done if it is raining.

c. Rain Amount. The total rain that accumulated during the period of chart recording--or more often--is measured. The use of a standard Weather Service inner cylinder of the 8 in. gage, or the use of a graduated glass cylinder, is recommended. This information, either as a total for the entire chart or as several separate readings are entered at the end of the applicable chart and on the chart box. After measurement, the water is dumped.

d. Site Examination. The gage should stand vertical with opening horizontal. The windshield around the gage should show no sag. If the site owner wants

the grass mowed in gage area, it is preferred that we do it to be sure no damage is done to the equipment.

e. Visits and work done are recorded on the metlog."

"5. The PD will attend a special 1400 weather briefing at the Wallops main station. He will be advised of the likelihood of showers during the afternoon and evening of that day. He will study the latest synoptic chart, radiosonde and other aids to help guide the experiment for that day.

6. He will proceed to SPANDAR to organize the operation. His decisions from this point onward will be determined by continuing study of the PAXFAX, SPANDAR PPI Polaroid sliced photos showing the progression of the storms and the sliced video Polaroids along with continuous contact with the Wallops station weather forecaster. SPANDAR PPI scans at a 2 deg elevation angle will be made at least every half hour when precipitation is predicted.

7. The PD receives various materials from the National Weather Service Office, Wallops Island, as indicated in the Facilities request. If the material is hardly legible, or missing, he should attempt to get suitable copy from the Weather Service. Checks should be made that each item is dated. Each day's records should be put in separate folders.

8. The PD will maintain the metlog. A form will be provided for this purpose. While all indicated items on the form would be complete, entries on where and when rain or showers are observed on the radar should also be included plus whatever the PD regards as significant, of special interest, etc. The log plus other material of each day should be placed in dated folders and checked that all the material has been collected into the folder. Chart rolls, film and cassettes are kept separately and with the folders are brought to APL by the PD."

Other aspects of the meteorology program will be discussed in Section 4.

3.3 RESOLUTION, ACCURACY AND CALIBRATION

This section describes features of the equipment relating to resolution and accuracy. Considerable emphasis was placed on these aspects since the goal was to have an overall system accuracy of better than $\pm$ 5 dB. At the end of this section it is shown that calibration, stability and processing errors were $\pm$ 4.05 dB peak and less than 1.65 dB standard deviation for this experiment.

3.3.1 Spatial Resolution

The overriding consideration in the selection of the SPANDAR radar for this program and the processing and recording techniques was the preservation and exploitation of the high spatial resolution available. The spatial resolution cell is defined to be one radar beamwidth in azimuth or elevation angle by one pulse length in range. The radar calibration included detailed beam pattern measurements so that the actual beamwidth is known, Ref. 32. The nominal width of the radar beam along with the aspect ratio of the spatial resolution cell as a function of range are shown in Figure 3.6. The 1 μs pulse length was chosen to take full advantage of the beam dimensions at close range. Note that the minimum observable range was 10 km due to ground clutter. At long ranges the beam becomes quite wide, e.g., around 1 km at 140 km range and the aspect ratio is also large. The effect of this beam-broadening on the accuracy of the reflectivity measurement is discussed later.

3.3.2 Dynamic Range

In this program it was critical to have the capability of measuring the very large reflectivities associated with hail-producing thunderstorms. The largest reflectivity values recorded are near 10^7 mm^6/m^3 (Donaldson and Tear, Ref. 35). The radar and processor had to be able to measure Z values of this magnitude at close range to ensure against the loss of a rare but extremely important event. On the other hand, the dynamic range of the radar also had to be wide enough to allow detection of less intense rain at 140 km.

The system dynamic range was determined by the log IF amplifiers. As mentioned earlier, the extended range log IF amplifier had a linear range of 90 dBm.

The variation in power received as a function of range and the equivalent reflectivity factor was shown in Figure 3.3. The radar

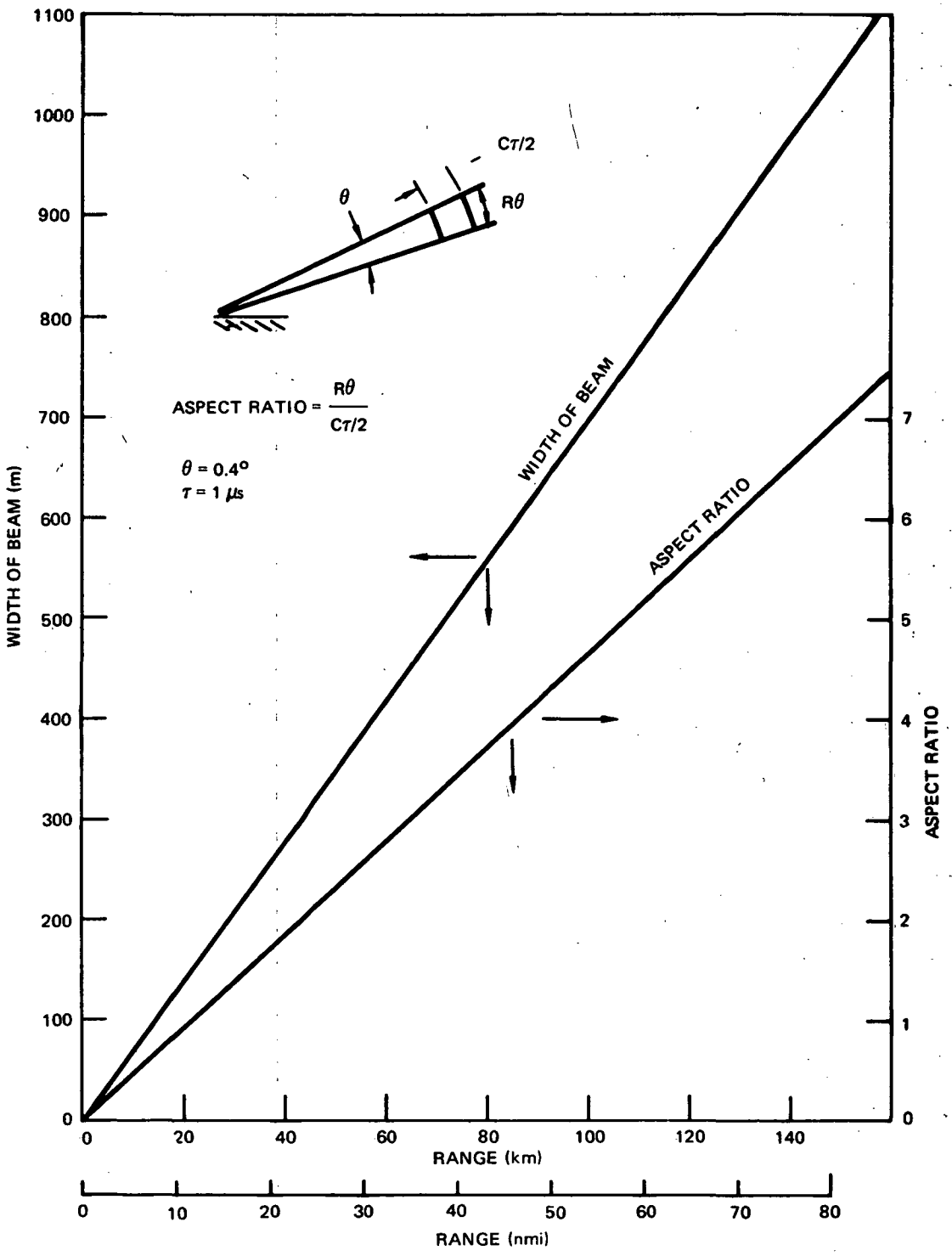

Figure 3.6. Beam Width and Aspect Ratios for Various Ranges

constant, k, and the antenna beamwidth, θ, are nominal values. The actual values were determined by the calibration program described later. Also included in Figure 3.3 is a plot of equivalent reflectivity factor vs rain rate for several measured Z-R relationships. The figure shows the range of the different parameters which can be measured in the manner described below.

A conservative estimate of the radar noise level is about -98 dBm (without the paramp). This assumes a noise figure of 10 and a 4 MHz bandwidth throughout the system. The true noise figure was determined by calibration during the experiment. Setting the lower limit of the linear range of the IF amplifier at a power received of -95 dBm just above the system noise, and allowing 10 dBm for fluctuations in the received signal, the lowest average power received which could be measured with confidence is -85 dBm. At the 140 km range, then, the minimum reflectivity factor is 27.5 dB. If one assumes, for example, the Joss model for thundershowers, the minimum rain rate which could be measured at the maximum range is approximately 1 mm hr^{-1}.

The upper limit of the 90 dBm linear range of the IF amplifier was at -5 dBm. Again allowing 10 dBm for signal fluctuation, the maximum average power received that could be measured with confidence was -15 dBm. This corresponds to a maximum measurable reflectivity of 75 dB at the closest range for which data were recorded, 5.4 nmi (10 km). Thus, the 90 dBm dynamic range of the log IF amplifiers covered all the reflectivity factors and rain rates of interest.

3.3.3 Measurement Resolution

The incoming radar video is first digitized to 6 bits by the A/D converter in the on-line data processing system. For a 90 dBm range of signal levels (discussed in the previous section), the quantization step size is 1.4 dBm (=90 dBm/64). The output of the integrator is an 8 bit word so that the output resolution is 0.35 dBm (=90 dBm/256). The uncertainty in the integrated power received due to the above truncations or quantizations is discussed in the section that follows.

3.3.4 Data Accuracy and Precision

The various sources of error contributing to the overall accuracy and precision of the radar measurements are discussed in the sections that follow. The estimated individual errors are worst case estimates and are not likely to be exceeded. Their sum is, therefore, a most conservative error estimate since individual statistical errors

will tend to cancel to some extent and systematic errors may be accounted for in data reduction.

3.3.5 Statistical Error

An extensive discussion on the probability distributions of fluctuating echoes from randomly distributed scatters has been given by Marshall and Hitschfeld (Ref. 16). Only the pertinent results will be given here.

Fluctuations occur in meteorological targets having constant reflectivity because the reflectors move with respect to each other and the phases of their backscattered signals change in a random fashion. An estimate of reflectivity can be obtained by averaging a number of independent echoes. The accuracy of estimated echo power, J_k, depends on the number of samples included in the average. The distribution of the average k samples, J_k, around the true value, $\overline{A^2}$, is given in Figure 3.7 taken from Ref. 16. These curves were derived analytically for A^2. However using a Monte Carlo technique they show that these same distributions are appropriate for log A^2 which is too complicated to handle analytically. Figure 3.8, derived from Figure 3.7 gives 50%, 80% and 95% confidence limits for the average k samples of log A^2 to be within ε of the true value. For example, an average of 100 samples of log A^2 falls within $\pm$ .4 dB of log A^2, minus a known constant, 80% of the time. Note that the accuracy improves very slowly for values of k greater than roughly 60. The RVP system integrates 128 independent pulses in the average received power that is recorded. Thus, the statistical error in the recorded data from this source should be slightly less than the $\pm$ .4 dB quoted above.

3.3.6 Quantization Error

A digital video integrator was used in the RVP system. Therefore, the errors introduced by quantization of both the integrator input, log A^2, and the integrator output, log $\overline{A^2}$, must be estimated.

Austin and Shaffner (Ref. 36) have considered the effect of quantizing the input to a digital integrator. It is shown that the logarithmically quantized average depends on the width of the quantizing intervals, and to a much lesser extent, the position of the true mean intensity within an interval. Thus they arrive at a relationship between input quantization error and the width of the intensity level interval. Figure 3.9 shows this relationship. Note that the error for no quantization whatsoever is -2.5 dB which agrees with Marshall and Hitschfeld's result (Ref. 16) for the difference between log A^2 and log $\overline{A^2}$ for analog

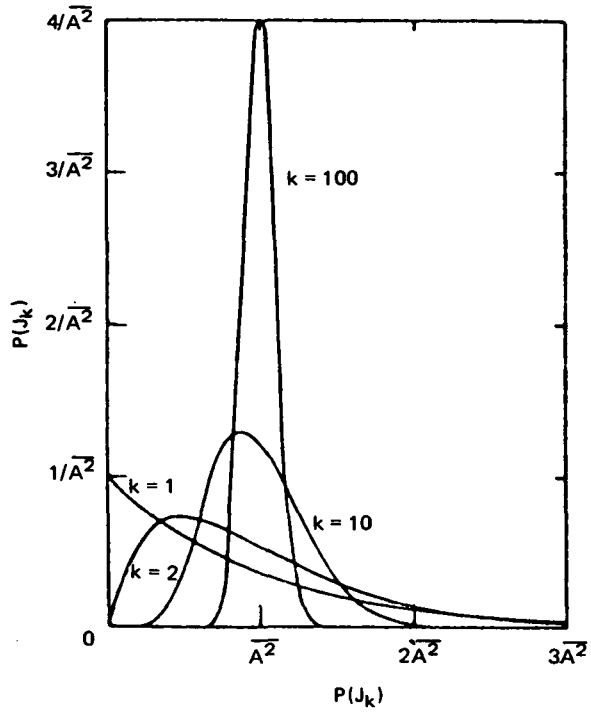

Figure 3.7. Probability Distribution of J_K vs $\overline{A^2}$

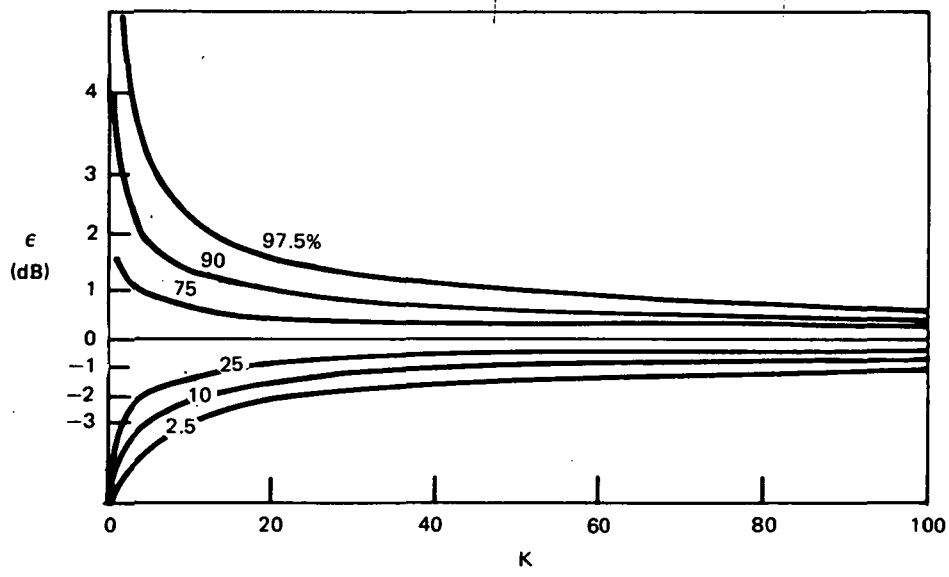

Figure 3.8. Confidence Limits for the Average of K Values of A^2 or Log A^2

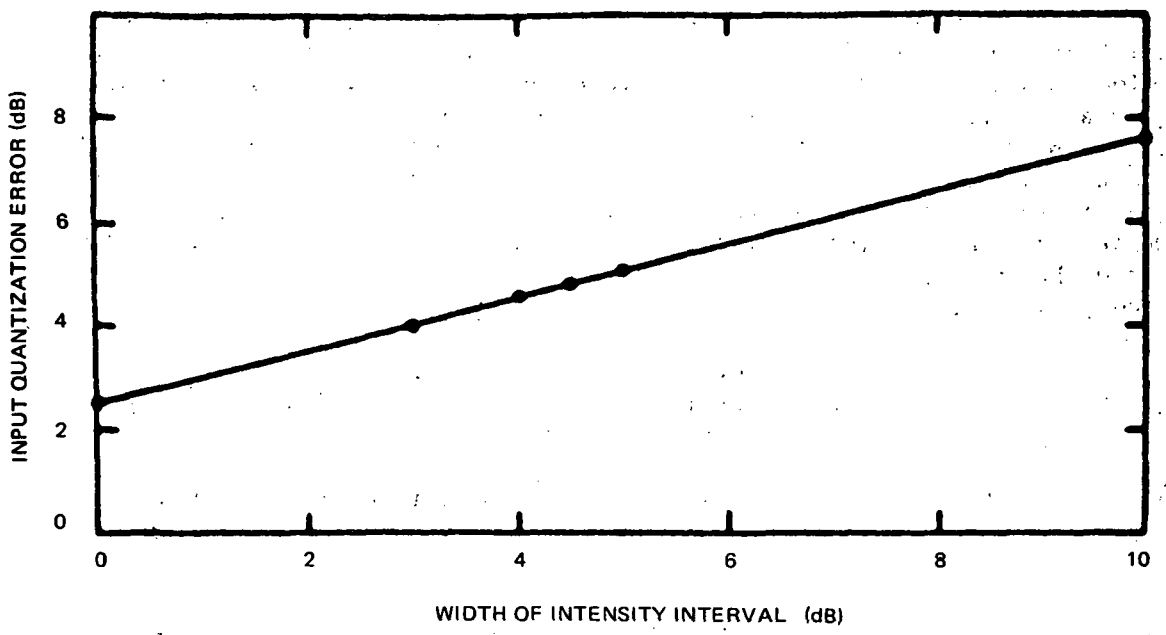

Figure 3.9. Error Due to Input Quantization

averaging. The assumption implicit in this discussion is that all statistical fluctuations have been smoothed by including a very large number of samples in the average. Therefore, if the appropriate correction is selected from Figure 3.9, the error from the quantization of log A^2 at the input to the integrator can be corrected completely. For the 1.4 dBm quantization step size in the A/D converters the input quantization error (or correction) is 3.2 dBm.

The maximum error contribution from the quantization of the integrator output is simply the value of the least significant bit. The output of the integrator was quantized into 256 levels over a dynamic range of 90 dBm so that the output quantization and, thus, the maximum error was 0.35 dBm.

3.3.7 Error Due to Reflectivity Gradient

An additional error is introduced when samples from a log receiver are averaged when the radar sample volume contains a reflectivity gradient. The conventional probability distributions for scatterers uniformly spread across the pulse volume (Ref. 16) are distorted when such gradients are present. Both the variance and the mean are affected in the case of log averaging.

This effect has been analyzed by Rogers (Ref. 37) for two different reflectivity gradient models; model 1 assumes a linear variation in log I across the pulse volume and model 2 assumes a linear variation in I. Model 1 is believed to be the most realistic. The relevant results of this analysis are presented in Figure 3.10 which shows how the estimates of variance and mean depend on the gradient parameter k. This parameter is the ratio of the power received from the most strongly reflecting region in the pulse volume, I_2, to the power from the weakest reflecting portion, I_1. Other parameters in the figure are defined as follows:

J = the average of log I for scatterers having constant reflectivity (equal to I_o, an average across the gradient).

$\langle J \rangle$ = the estimate of log I obtained from an average of log I when a gradient is present across the pulse volume.

σ_j^2 = signal variance for scatterers having constant reflectivity $\langle I_o \rangle$.

Σ_j^2 = the measured signal variance of log I when a reflectivity gradient is present.

Gradients of 20 dB/km are not uncommon in thunderstorms. Such a gradient located at 140 km from SPANDAR represents a worst case situation. The beamwidth at that range is about 1 km so that a 20 dB variation in reflectivity will be used in this example. The curves evaluated at the corresponding k value, 100, shows that a bias of 3.2 dB is introduced, and the variance is increased by about 3 dB for the more representative model 1. Thus in this worst case one would underestimate the Z value by about 3 dB, and the statistical uncertainty of .4 dB for the uniform distribution of reflectors increases to about .8 dB or less for 80% of the time. Note that these errors improve significantly at distances of about 65 km where k reduces to 10 for a 20 dB nmi^{-1} gradient.

Although the foregoing shows that errors of 3 dB or less are possible in regions of high gradient, the Z value of most interest, i.e., its maximum value, will be least affected by this type of error.

3.3.8 Integration Error

An error contribution is produced by the integration of N independent pulses as the beam sweeps through the target. If we assume

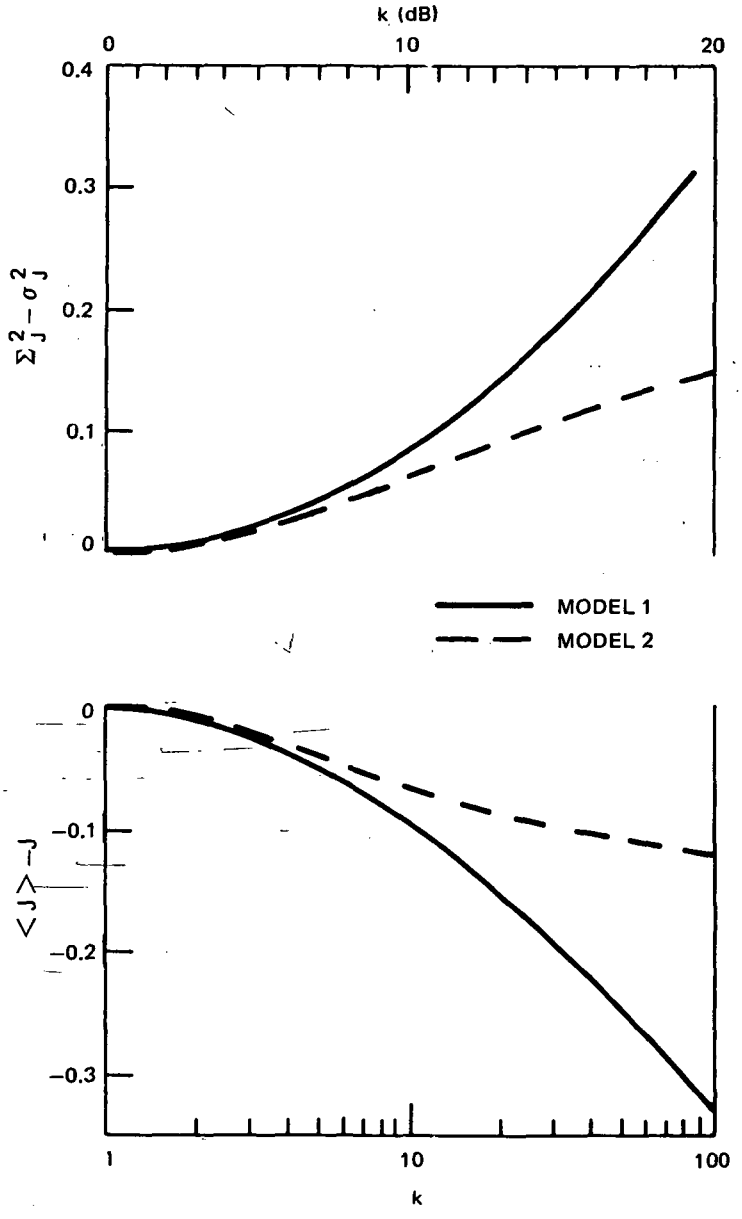

Figure 3.10. Effect of Nonuniform Reflectivity on the Mean Value and Variance of Signal Intensity Level

a true averaging (rectangular weighting) digital integrator, the output of the integrator is

$$\bar{\varepsilon}_o = \frac{1}{N} \sum_{i=0}^{N-1} \varepsilon_i ,$$

where ε_i is the i^{th} input to the integrator in dBZ. Donaldson's (Ref. 56) storm profile for model 1 is of the form

$$\varepsilon = dBZ_m - mX^2$$

where dBZ_m is the dBZ value in the storm core, m is the constant defining the apparent storm size as observed with a finite beam, and X is the distance from the storm center. The i^{th} input to the integrator will be the sum of the mean Z value at a distance $i\omega RT$ from the thunderstorm core plus a noise component, n_i. With no loss of generality the assumption is made that the beam is directed at the storm center for the sample i = o. In the above, ω is the scan rate in rad/sec, R is the range, and T is the time between independent samples. Thus, the i^{th} input to the digital integrator becomes

$$\varepsilon_i = dBZ_m - m(X-i\omega RT)^2 + n_i$$

so that

$$\bar{\varepsilon}_o = dBZ_m - \frac{1}{N} \sum_{i=o}^{N-1} (X-i\omega RT)^2$$

since

$$\frac{1}{N} \sum_{i=o}^{N-1} n_i = 0.$$

Carrying out the sum produces the result,

$$\bar{\varepsilon}_o = dBZ_m - m \left[X - \frac{1}{2} \omega RT(N-1) \right]^2 \frac{1}{12} \; m(\omega RT)^2 \; (N^2-1)$$

which shows a bias error of

$$\delta\bar{\varepsilon}_o = -\frac{1}{12} m(\omega RT)^2 (N^2-1)$$

and a displacement error of

$$\delta X = \frac{1}{2} \omega RT(N-1).$$

Worst case values for the present experiment are as follows:

ω = $360^o/92$ sec $\cong$ .07 rad/sec

R = 140 km

T = 10^{-3} sec

N = 128

m $\approx$ 1 dB/km^2 (Ref. 56).

These values lead to

$$\delta\bar{\varepsilon}_o \sim .2 \text{ dB},$$

and

$$\delta X \sim .6 \text{ km},$$

both of which were acceptable for the present experiment.

3.3.9 Beam Shape Error

Extensive work has been done by Donaldson and Tear (Ref. 35) and Donaldson (Ref. 56) in estimating the effect of smoothing by the radar beam. Functions representing seven storm profiles were convolved with an idealized beam pattern to provide the smoothed profiles used to estimate distortions in cloud profiles and errors in Z measurements.

Extrapolations from the results of Donaldson and Tear (Ref. 35) indicate that a $.5^o$ beam would contribute errors in the measurements of maximum Z value of less than 2 dB at 100 km range and less than 4 dB at 200 km. The seven models used were typically about 4 or 5 km in size at their 3 dB points. Therefore, it is believed that variations in cell reflectivity across the beam only infrequently result in Z_m errors greater than 2 to 3 dB in the vicinity of 150 km.

Severe distortions can result in the measured storm profiles at distant ranges because of the finite beamwidth. Results for Donaldson's model 1 (Ref. 55), one of his most realistic, are shown in Figure 3.11. The figure shows the effect at longer ranges of the side lobes illuminating the intense core when the main beam is well above the storm top. For this reason, accurate measurements of storm height should be performed only at a close range and with a narrow beam radar. Note that for this model contours as much as 5 dB below the measured Z_m value are not strongly dependent on range.

The beamwidth for SPANDAR is 1.0 km across the 3 dB points at 140 km range. This is the maximum acceptable range that would enable a rather small cell of about 3.5 km diameter at points 3 dB down from Z_m to be measured with acceptable resolution and accuracy.

3.3.10 Radar Stability and Accuracy

The nature of the rain cell statistics program in which radar reflectivity is measured and transformed into rain intensity levels required that every possible effort be expended in calibrating the radar sensor for absolute measurements. This requirement for accuracy of measurement is commensurate with the fine spatial resolution available at SPANDAR with its 0.4 deg beam and 1 μs pulse length.

Since measurements were taken over an extended period of time, the drift and stability of the sensor (the radar system) was important both on a short-term (hours) and a long-term (months) basis. Observations taken during a given sequence of scans had to be accurately relatable to each other and to other series taken several months apart.

The calibration program for the SPANDAR radar is outlined in Table 3.1. There were two major elements in the program, the pre-experiment program and the during-experiment program. The pre-experiment program was primarily concerned with the measurement of system characteristics, e.g., antenna patterns, gain, transmitter bandwidth, power, transmission losses, receiver noise figure, bandwidth, etc. The details of this program are contained in Vann (Ref. 32). Preliminary results are in Vann (Ref. 27).

In establishing an accuracy figure for the radar, attention was given to the following:

a. Location at which the calibrating signal is injected

b. Location where the measured gain is referred

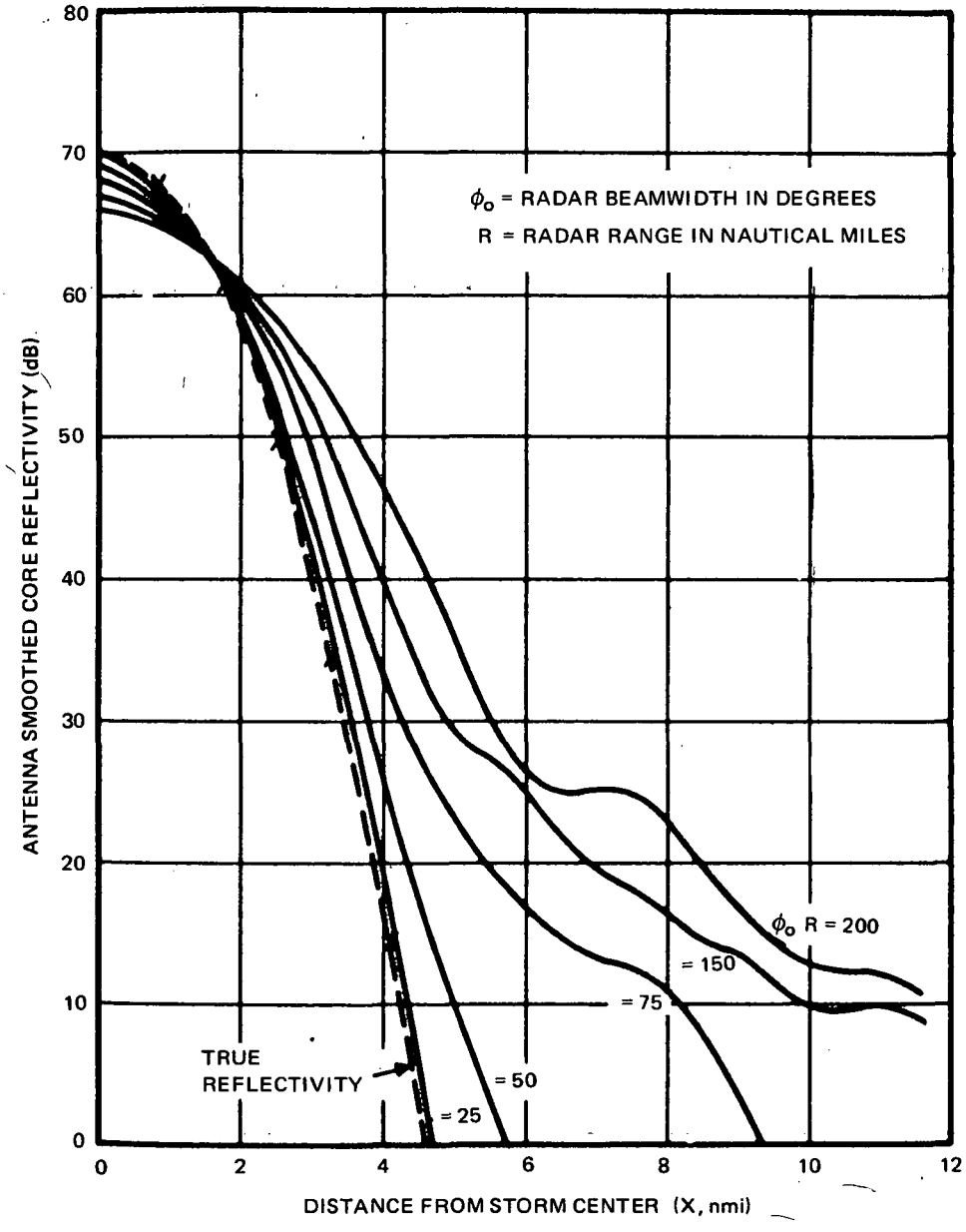

Figure 3.11. Effect of Beam Smoothing on Donaldson's Cloud Model 1 (Ref. 56)

Table 3.1

Calibration

A. INITIAL MEASUREMENTS

1. Confirm Linearity of Polarization
2. Measure Line Losses Including Rotary Joints
3. Measure Antenna Gain and Pattern
4. Measure Receiver Gain and Bandwidth
5. Design and Fabricate a Method for Finding Scanner Position When Stopped

B. PERIODIC CALIBRATIONS

1. Use Boresight Tower
2. 6 in. Sphere

C. DAILY CALIBRATIONS AND TESTS

1. Measure Minimum Detectible Signal
2. Monitor Transmitted Power and Pulse Shape
3. Set Up Log Strip
4. FR-910 Check for Optimum Operation
5. Test RVP; CW Signal with Ramp to Test All Bins and All Steps in Each Bin; Use Automatic Stepped Attenuator

D. CALIBRATION AND TESTS FOR EACH RUN

1. Transmitted Power
2. Frequency Diversity Check: Deviation and Power

E. CONTINUOUS CALIBRATIONS AND CHECKS

1. Transmitted Power
2. High Level Signal
3. Low Level Signal
4. Receiver Noise (Scope Monitor)

c. Accuracy of the gain measurement

d. Accuracy of the measurement of insertion loss between the locations where the gain is measured and the calibrating signal is injected

e. Stability of the transmitted power and the accuracy of the calibrating signal.

The calibrating signal was a sample from the transmitter input and the accuracy of the losses in the couplers and associated lines had to be measured. Since this calibrating signal was injected into the mixer input of the receiver, gain instabilities and losses in the receivers influenced the incoming signals in the same way as the calibrating signal. Hence, the characterization of the receiver properties played a minor role in the accuracy question.

Since frequency diversity was used, the variation in transmitted power as a function of frequency had to be measured. The VA-57 klystrons used in the FPS-18 transmitters could be tuned to be uniform in power to within 3 dB over a 25 MHz frequency range. The slight reduction in average transmitted power due to frequency diversity was taken into account in system calibration.

The second part of the calibration program concerned the monitoring and/or logging of critical points in the radar system during the experiment. Certain parameters such as transmitted power, calibration levels, and receiver noise were monitored and recorded continuously. Other items were checked and/or logged less frequently such as daily or weekly. The details of these measurements are contained in Ref. 32.

3.3.11 Calibration

The calibration program comprised a number of measurements which may be divided into the following major phases:

Phase 1: Pre-program measurements performed before the rain measurement program was initiated.

Phase 2: Measurements performed before, during, and after each rain measurement day.

In the following paragraphs, a description of the types of measurements, and the procedures followed are given for each of the phases and references are given to applicable memoranda characterizing the associated measurements.

3.3.11.1 Phase 1 - Pre-Program Measurements. The aims of this phase were to establish the operating characteristics of SPANDAR as well as to enable a subsequent system of monitoring to achieve a high level of accuracy during the experimental period. A complete report on these efforts is given in Ref. 32 and is included in this Final Report as Appendix C, Volume III.

Specifically, a large number of measurements were made covering the transmitter, antenna, and receiver along with the associated waveguide transmission lines, monitoring couplers, coax lines and attenuators. The measurements were performed initially to determine the general condition of the microwave system and to identify any component that had to be replaced due to high VSWR or insertion loss. The measurements were then repeated after replacing several sections of waveguide.

Some concern had been expressed regarding the second and third time around rejection of radar returns due to the frequency separation between adjacent pulses. In order to provide this information the radar preamp response was measured and the entire receiver chain was measured over an extended frequency range at signal levels covering the full dynamic range of the system. A subsequent analysis (Ref. 38) demonstrated that second-time-around errors could be neglected.

The FD chassis was a key element in the experiment and a large number of tests were performed on the unit in order to determine the stability, frequency linearity, power output variations across the frequency band and the stability of the timing system (Ref. 14). Some problems were observed in the timing system stability and the circuitry was modified to a counter-controlled delay generator with a much improved stability.

Extensive antenna patterns were measured covering the principal planes at several frequencies, along with backlobe and spillover lobe response and a set of stepped elevation patterns were obtained from which antenna contours were generated. Antenna gain measurements have been reported in Ref. 30.

A system of continuous monitoring and calibration was devised for the SPANDAR radar which consisted of continuous measurement and recording of certain parameters, periodic measurement of other parameters, periodic injection of a known level signal from a source external to the radar, continuous injection of noise samples and samples of the transmit frequency timed to occur in the radar dead times. These are alluded to in the description of Phase 2.

3.3.11.2 Phase 2 - Measurement Program During Experiment. The calibration program followed is essentially that outlined in the operations plan described in the Operations Test Plan, Ref. 13. The FD unit represented a vital component of the system and hence the continuous monitoring of this unit was considered essential for guaranteeing the validity of the experimental results.

Figure 3.12 is a block diagram, which among its other features describes the various outputs of the FD chassis and how this unit relates to the other components of the radar system. Also shown in this diagram are the nominal power levels and pulse widths at the various outputs of the FD chassis and at the other stages of the system. The major procedures and the associated calibration results are listed in the following paragraphs where references are made to the numbered components [ ] of Figure 3.12.

1. Before each rain measurement day, a known test signal was injected daily into a standard gain horn on the 250 ft meteorological tower at Wallops Island and the received power at the mixer input was monitored. Such measurement represented a daily check of possible fluctuations of the antenna gain and line losses down to the mixer input. The fluctuations observed during the entire summer varied peak to peak within $\pm$ 0.3 dB of a given average level. A description of this test is given in Ref. 30.

2. Step calibrations of the receiver-processor system were performed in 3 dB steps over a 90 dB dynamic range (-100 to -10 dBm) before, during, and after each rain measurement day. The outputs, in digital form, were monitored in real time on the teletype and simultaneously plotted to establish the existence of possible anomalous effects or deviations from logarithmic linearity. On occasion, when such anomalies were observed, they were subsequently corrected before continuing with the experiment. The system linearity was found to be well within $\pm$ 1 dB throughout the entire season.

3. The forward and reflected power, [5] and [6], as well as the High Cal. Monitor, [9], were continuously monitored with a strip chart recorder during the entire rain measurement day. The transmitted power was found to fluctuate within $\pm$ 0.1 dB relative to a peak power of 1 MW (as referenced at the power output monitor). The calibrate output fluctuated daily within $\pm$ 0.2 dB, although a long-term drift was observed. This drift was accounted for by noting its daily level and adjusting the FD unit to give a constant calibrate output.

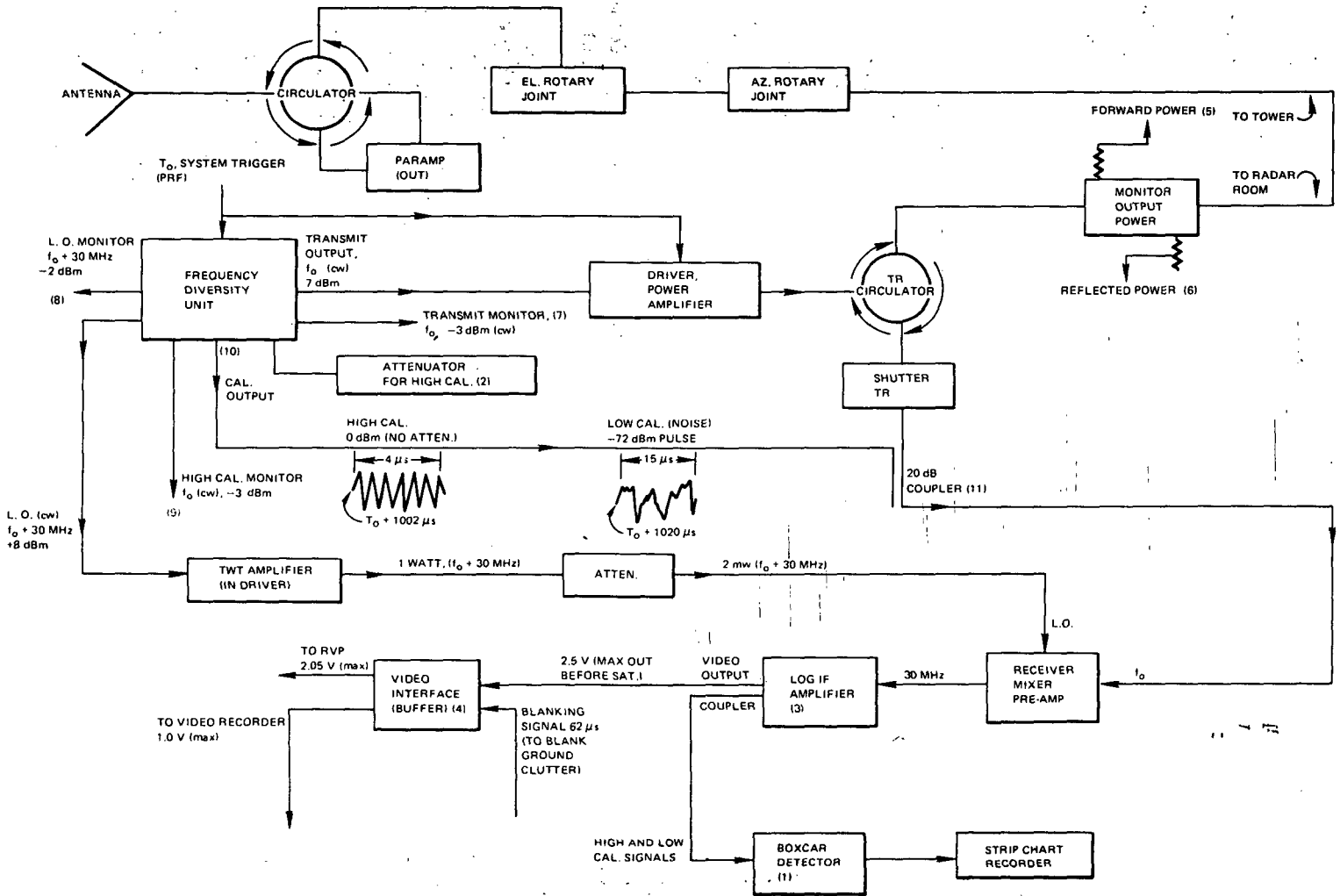

Figure 3.12. Block Diagram of Pertinent Components of SPANDAR with FD Chassis

4. During each one-half hour interval the following levels were logged.

   a. Local oscillator crystal currents

   b. Forward and reflected power [5] and [6]

   c. FD chassis LO monitor output [8]

   d. FD chassis High Calibrate Monitor output [9]

   e. FD Transmit Monitor [7]

   f. High and Low calibrate video outputs (output of [3])

   g. Center frequency, f_o.

The above records were examined daily for diagnostic purposes to establish the extent of any deviations from the nominal levels. In general, all levels remained sufficiently close to their nominal values during the entire rain program.

3.3.11.3 Calibrate and Noise Signals Recorded on Tape. Averages of 128 samples of the high and low calibrate signal as well as receiver noise were recorded continuously on digital tape in defined bins associated with each transmitted pulse. The high calibrate signal is at a frequency, f_o, with the leading edge occurring at a time, t_o + 1002 μs (t_o = time of leading edge of transmitted pulse), the pulse width is 4 μs and the pulse power is 0 dBm (assuming zero attenuation at [2]. The low calibrate signal is a noise pulse whose leading edge occurs at a time, t_o + 1020 μs, has a pulse width of 15 μs, and a power level of -70 dBm (average power over a pulse). The output is at the same location as that of the high calibrate pulse [10]. The combined signals are injected into the receiver mixer through a 20 dB coupler [11] resulting in power levels of -20 dBm and -90 dBm, respectively, at the mixer input terminals.

These averaged high and low calibrate signals were used in subsequent programs to establish intermediate power levels through interpolation procedures. This calibration scheme allowed for the compensation of either short- or long-term receiver gain changes.

3.3.11.4 Radar Calibration Constant and SPANDAR Error Budget. In Ref. 30 are described the measured parameters of SPANDAR which appear in the radar constant. In addition, the total error budget is derived and the uncertainty in the reflectivity factor, Z, established. Although these

error uncertainities were in part based on initial measurements during the early stages of the rain statistics program, subsequent measurements resulted in uncertainties consistent with the earlier levels.

The resultant reflectivity factor as extracted from the radar equation was shown to follow the relation,

$$Z(dB) = P_{ri}\ (dBm) + 20\ Log_{10}\ r(nmi) + L_a + K_i \qquad (1)$$

with,

$$K_i = 76.3\ dB \qquad (2)$$

where P_{ri} (dBm) represents ten times the logarithm of the average power expressed in dBm. This quantity was extracted from the average of the logarithmic power through the addition of a 2.5 dB correction term.

An additional 0.9 dB has also been added to correct for quantization errors, see Ref. 30. K_i in (1) represents the resultant radar constant which accounts for the correction in P_{ri}, transmitted power, gain, receive and transmit losses, wavelength, beamwidths, rain refractive index, pulse width and any associated constants. r(nmi) represents the range (expressed in nautical miles) and L_a represents the two-way atmospheric absorption primarily due to collision broadened resonances of the oxygen molecules. This quantity is dependent upon the range of the target and elevation angle of the beam. This term may give levels as high as 2 dB (for grazing angles at 140 km range) at S-band and was accounted for using a CRPL exponential reference atmospheric model (Ref. 28).

3.3.12 Error Summary

In Table 3.2 is given a summary of the error budget (extracted from Ref. 30).

The first column lists the peak error levels and the second the upper limit values for the standard deviations. The radar calibration stability errors include the uncertainties in the gain, line losses, beamwidths and transmitted power. The processing errors include the uncertainties in the system linearity, output quantization, statistical averaging and interpolation due to instabilities of the high- and low-calibrate signals. The phenomenological errors include: beam smoothing (associated with the smoothing by the nonuniform beam pattern of the reflectivity profile); integration errors (associated with the integration of 128 pulse occurring simultaneously as the beam sweeps through

nonuniform scattering regions); reflectivity gradient errors (associated with the averaging of the logarithm of the power for cases in which the radar pulse volume contains a reflectivity gradient); and the absorption error (associated with the uncertainty on the modeling of the O_2 correction term).

Table 3.2

Error Summary

	Peak	S.D.
1. Radar calibration and stability errors	2.0	1.0
2. Processing errors	2.05	1.3
Total peak of (1) and (2)	4.05	
Resultant Standard Deviation (1) and (2)		1.65
3. Phenomenological and other uncertainties	-2.5 ± 0.2	

4. METEOROLOGICAL CONSIDERATIONS

Weather entered the rain statistics program in several ways. It was of prime consideration in carrying out the experiment properly, i.e., the Project Director needed accurate forecasts for planning and he needed a knowledge of the present weather pattern during daily operations. Then, of course, he required measurements of the presence of, and amounts of, rain during the course of radar data accumulation. In addition, for analytical purposes after the experiment, the analyst needed temperature, moisture, wind and precipitation information in three dimensions and changes of these parameters with time. With these the analyst could categorize the rain structure to carry out the important task of extending the statistical measures of rain cells to other climatological regions.

This section discusses some relevant features of precipitation, their characterization and what was needed to carry out this

effort in the present experiment. More detail along those lines will be found in References 39, 40, 41 and 42.

4.1 RAIN CHARACTERIZATION

There were many rain characterization schemes in use or suggested. For example, Austin and Houze (Ref. 43) used the division: large mesoscale areas, small mesoscale areas and cell. Austin (Ref. 44) used thunderstorm rain and nonthunderstorm rain for characterization (and includes rainfall rate observations). Rice and Holmberg (Ref. 45) used a thunderstorm and nonthunderstorm characterization (and included geographic climatic regions).

It was necessary that meteorological quantities that might be used be available. Thus, while drop-size distribution aloft was the best quantity, it was unfortunately unavailable.

The meteorological quantity most often used is R, the rain rate, which is both available and numerical. In addition to being related to the reflectivity factor, Z, rain rate has another useful feature - information can be obtained on the probability of occurrence of various rain rates. It is this feature of R that makes it most useful in microwave communication, although this feature is of lesser interest to the radar meteorologist. There was, therefore, a third requirement for the meteorological data - that it be potentially capable of providing probability estimates.

For the purpose of microwave propagation and communication, there are specific expectations to be provided by a rain characterization. However, it is not a priori apparent that a specific characterization of a rain type (say, nonthunderstorm) would optimally describe the statistics of the reflectivity factor, and the statistics of area, and the statistics of height distribution, and the statistics of intercell distance, etc. The question faced was if one characterization does not describe these well, what alternative characterization does, bearing in mind that only a practical scheme was acceptable.

There are at least two approaches to a characterization. In one approach separate classes are identified such as thunderstorm and nonthunderstorm, or alternatively the classes: thunderstorm, warm front rain, cold front rain, squall line rain, etc., are identified and the statistics of each class determined. While the identification into classes did not meet the desire that it be numerical, it was nevertheless acceptable. In the use of rain types or classes, it is obvious that the class definition be unambiguous. This was a real problem. Austin (Ref. 44) was careful to define what she meant by "thunderstorm rain." It had to meet the criterion that at least one of four observing

stations, within 40 mi, report thunder on the day that the rain occurred. In discussions sponsored by CCIR the term "excessive precipitation" is used to identify rain as "thunderstorm rain." There is a need for arriving at a common, acceptable definition. There are further complications in the case where a rain meets the definition of two classes. Suppose there are some thunderstorms embedded in a squall line. Some priority would eventually be needed for assigning this rain to one particular class, or a decision reached on how to classify such cases. Another approach to characterization was to select a set of (plausible) meteorological parameters in addition to some of the above rain typing, and by regression or otherwise relate these to Z, if indeed there are significant correlations. The statistics would then be about some model relation between Z and other parameters. Probability estimates would use the probability of occurrence of different values of these parameters, singly or jointly as the model indicates. By this approach it may be possible to coalesce some rain types, e.g., thunderstorm and nonthunderstorm convective shower, into single types or the numerical equivalent of these types.

In the statement that there are other "meteorological parameters" of potential interest in categorizing rains, note that these were largely available from routine meteorology, and thus obtaining them did not pose a significant burden on the program.

4.2 ELEMENTS IN RAIN CATEGORIZATION

There was a body of knowledge available to aid in identifying rain classes and parameters. Local influences which can impact on the analysis are also considered in this section.

4.2.1 Physical Considerations

The physics of precipitation, although incomplete, may provide clues to the meteorological quantities more likely to be useful. The phenomena that lead to the growth of raindrops are condensation on the precipitation particle and collision (accretion, coalescense). In addition, lifting of the moist air, which then cools, is needed. Upward air movements occur at different rates. In a warm front situation air is lifted slowly and drops grow principally by condensation. In a convective situation there are faster upward air movements and with droplets of different size and with different velocities there is an accentuated relative motion between the larger and smaller drops enhancing the growth of the larger drops by collision with the smaller drops. If, in addition, there is small scale turbulence the growth possibility by collision is further enhanced. There are processes that cause drops to decrease in size. There is evaporation and also drop break up if it

becomes so large that it distorts and breaks up, or if the outer layer freezes followed by the frozen shell breaking and releasing the drop interior as smaller drops. The probability of finding an ample supply of large drops, and thus higher Z, depends on having several growth processes occurring while drop diminution processes are of small importance.

Even though the foregoing discussion is simplistic it does point to categorization schemes, to the identification of desired parameters and to potential concerns in interpretation of results. For aid in categorization there are data available from rawinsonde flights, from data transmitted on Weather Service circuits and from some special local measurements. The relationship between the requested information and the physically significant information may be indirect; for example, an estimate of the relative intensity of the vertical velocity is obtained from the air "stability." There is a potential concern that the transformations between Z and R and attenuation and similar quantities presume a certain drop size distribution. However, the discussion of the preceding paragraph suggests that the drop size distribution may differ, even possibly in the functional form, for different rain situations. Thus, we can intuitively expect more larger drops (higher Z's) in thunderstorms where there are pronounced vertical air flows, high moisture content in a cloud of large vertical extent and considerable small scale turbulence. In contrast, a hurricane may show the same rainfall rate but lower Z's as the small scale turbulence is less pronounced, and the repeated up and down motions that a drop undergoes in a thunderstorm is not common. Similarly, it may be possible to have the same Z's for different rainfall rates.

The above discussion relating to rain characterization and the physics of precipitation are meant to point out some of the important features relating meteorological parameters with the statistical description of precipitation as determined using radar. Although the radar analysis was to a large extent completed and documented in Volume II, a parallel effort was unfortunately not made in the meteorological area. Thus it yet remains to perform a definitive analysis to bring the meteorological aspects to a comparable position.

4.2.2 Local Considerations

In this section the meteorological situations which occur at Wallops Island and produce copious rains are identified. There are hurricanes and lesser storms of tropical origin; there are thunderstorms; there are coastal storms. The latter include lows that are near the coast, fronts that lie near the coastline and nearly parallel the coast;

such storms sometimes form as secondaries to a system located about 1000 km to the west. (Other areas of the world have their own types of rains--monsoon rains in India, coastal-orographic rains in Washington and Oregon.) In addition, there were, in the vicinity of Wallops Island, certain other local features. There is the ocean on the east, the relatively narrow (about 10 mi) strip of land to the west and the relatively broad Chesapeake Bay (about 30 mi) beyond. A convective type storm may need a continual thermal energy input from below to maintain itself. Passage over water could deny it an energy source. (There is still an energy source aloft from the heat release during condensation.) The growth/decay history of a cell might depend on where the cell was observed and on its movement. The sea-breeze phenomena might have influenced the results as there was an added vertical velocity field. Another local consideration was the existence of a fairly heavily travelled airway nearby. The production of contrails (ice crystals) could have led to an intensification of rain by cloud seeding.

4.2.3 Meteorological Descriptors

a. Qualitative description. Individual days were described in a qualitative manner including general synoptic situation. These descriptions contained such pertinent elements as sea-breeze, presence of cirrus, and general storm movement.

b. Rain rate. Quantitative measure of precipitation rate available from various rain gages.

c. Vertical extent of cloud

d. Horizontal extent of cloud

e. Stability measures. There are two stability measures currently distributed that are deducible from the radiosonde flight, the lifted index and George's K-index. These were available from the local sonde, teletype reports FOUS 1 and 2 and FOUS 10 and 11, and the facsimile composite moisture chart. The K-index, for example, has been reported to give the highest correlation with radar activity, according to the National Weather Service Technical Procedures Bulletin, No. 71, March 6, 1972. Another class of stability measures is the vertical velocity. This is not a measured quantity; it is computer-derived for the 700 mb level. It was obtained from the facsimile chart "Relative Humidity/Vertical Velocity," and from teletype reports FOUS 1 and 2, and FOUS 10 and 11.

f. Storm motion.

g. Moisture. Information on moisture-related quantities were available from several sources. There were the local and nearby sondes. Teletype reports FOUS 1 and 2 gave the mean relative humidity of the lowest 3 levels of the 6 level primitive equation model (surface to about 490 mb). It also gave the quantitative precipitation forecast. The composite moisture facsimile chart had "precipitable water" and the average relative humidity (surface to 500 mb), each computed from radiosondes. The relative humidity/vertical velocity facsimile chart had the mean relative humidity as in FOUS 1. There was also the heavy precipitation forecast transmitted on the FOFAX circuit.

h. Significant heights. There is a set of potentially significant heights/pressures from various sources. The use of pressures is motivated from thermodynamic considerations. The local and nearby radiosondes routinely report these. In addition the local sonde provided height and pressure of the -4°C level, the 0° level and the tropopause. The freezing level is also on the composite moisture facsimile chart, but it is noted that in the case of several freezing altitudes, only the lowest one is given. The tropopause is shown on the "Upper Levels/ Tropopause Data" facsimile chart.

i. Winds. Winds from local measurements and from nearby stations are given to several levels. While it has been reported that in the mean, the echo drift velocity becomes closest to the 10,000 ft wind, information for storms to varying heights may refine this. Consequently the analysts anticipated using the winds at 8,000, 10,000 ... 18,000 ft. It has also been reported that echoes move at a lower speed than the winds, with the lower speeds associated with the stronger echoes. This suggests an analysis which compares the difference between wind and echo drift with Z. Wind shear, the difference of wind between two altitudes, appears to have an effect on the vertical extent of shower clouds and storm intensity.

j. Temperatures. With the thought that the higher the temperature the greater is the amount of water the air can hold and with the observation that as one moves equatorward, toward the warmer temperatures, the thunderstorms extend to higher altitudes, (significantly,

there is a higher tropopause, too), the temperatures at selected standard levels are appropriate to the present experiment. These data come from radiosonde data and are given on standard level facsimile charts. A closely related quantity is the thickness of the surface to 500 mb region.

5. SUMMARY OF DATA

In this section are listed the data available from the various sources taken during the 1972 and 1973 experiments. The radar data and that appearing in photographic form are tabulated in Section 5.1. In the meteorological aspects all the data sources and the data that have been cataloged and are available at APL for analysis are listed. These are found in Section 5.2.

5.1 RADAR AND PHOTOGRAPHIC DATA

This section lists in tabular form all the data available from the spatial statistics 1972-1973 experiment.

For each day during which precipitation was observed the total number of each of the following is listed in Table 5.1.

1. Polaroid photographs.
2. 360 deg scans. Also, the number of such scans on Polaroid (P) and on digital tape (T).
3. 2 deg elevation PPI scans. (P) and (T) as above.
4. Raster scans.
5. Sweeps in all PPI raster scans on that day.
6. Average number of sweeps in each raster scan.
7. Individual RHI scans. (P) and (T) as above.
8. RHI raster scans.
9. Sweeps in all RHI raster scans on that day.
10. Searchlight mode observations.

Table 5.1
Radar Data Available from the Spatial Statistics 1972–1973 Experiment

	(1)	(2)		(3)		(4)	(5)	(6)	(7)		(8)	(9)		(10)	(11)	(12)	(13)
Date	Polaroid Photos	2° EL 360° Scans		Sector 2° PPI Scans		PPI Raster Scans	Sweeps in Raster Scans Total for Day	Average Sweeps Per Raster Scan	Single RHI Scans		RHI Raster Scans	Sweeps in RHI Raster Scans		Search-light	Digital Tape Numbers	Video Tape Numbers	35 mm Numbers
		P	T	P	T				P	T		P	T				
1972																	
9/15	39	15	15			2	24	12								1	738-786
9/18	95	23	2			6	65	10.38	7	7						2	
9/19	62	17	7			6	45	7.5	2	2						3, 4	
9/21	26	24	23	2	0											4, 5	
9/25	10	10	4														
9/27	154	33	19			9	103	11.44	4	2	1	14	14			5, 6, 7	
9/29	76	30	28			6	42	7	5	5						7, 8	
9/30	76	15	15			5	60	12	1	1						9, 10	
10/5	9	9	4													11	
10/6	16	6	6			1	10	10								11	
Total 10 Days	563	182	123	2	0	35	349	9.97	19	17	1	14	14				
1973																	
5/9	47	13	0			5	34	6.8							DV13	12	
5/14	62	13	0			5	47	9.4			1	3	0		DV13	12, 13	
5/15	39	16	0			4	22	5.5	1	0					DV13	13	
5/17	84	14	9	1	0	7	69	9.9							DV13	13, 14	
5/23	71	15	9	4	0	8	52	6.5							DV9	14, 15	617-687
5/24	133	17	3	3	0	13	109	8.4	4	2					DV9	16, 17	702-831
5/29	184	16	8	2	1	13	166	12.8							DV10, D2	18, 19, 20	863-1074
6/13	197	17	1	10	8	13	170	13.0							D6	21	1178-1363
6/18	196	14	0	15	15	13	167	12.8							D5	22, 23	1387-1587
6/20	34	15	0			2	19	9.5							D8	25	1658-1684
6/21	209	14	0	13	13	17	177	10.4	5	0					D8	24, 25, 26, 27	1690-1895
6/22	307	19	15			27	285	10.6	3	0					D8, 9, 10	27, 28, 29, 30	1903-2207
6/26	22	10	0			2	12	6							D10	30	2255-2271
6/27	113	16	4	3	2	7	94	13.4							D10	30, 31	2279-2390
6/28	45	15	0			4	30	7.5							D10		2391-2428
6/29	353	16	2	7	7	31	330	10.6							D11, 12	32, 33, 34	2435-2791
7/3	198	16	0			15	178	11.9	4	0					D12	34, 35, 36	2803-2991
7/5	55	12	0			6	43	7.2							D13	37	2995-3055
7/10	281	13	0	3	1	21	266	12.7							D13, 14	37, 38	3104-3385
7/11	175	11	6	2	2	17	161	9.5	1	0					D14	39	3397-3571
7/18	33	12	0			4	22	5.5	1	0					D15	40	3734-3760
7/20	60	14	0			4	43	10.75	3	0					D15	41	3835-3893
7/27	163	14	0	3	3	15	146	9.7	1	1					D15	42, 43	3910-4069
7/31	116	13	0	4	4	12	100	8.3							D16	43	4070-4179
8/1	225	12	1	11	11	16	170	10.6	2	0	3	32	32		D16, 17	44, 45	4179-4374
8/2	171	14	2	8	7	13	127	9.85	2	1	2	20	20		D17, 18	46, 47	4376-4528
8/3	225	17	10	5	5	19	186	9.8	2	1	1	15	15	2	D18, 19	47, 48, 49	4528-4727
8/13	277	13	1	11	9	27	252	9.3	1	0					19, 20, 21	49, 50, 51	4735-5010
8/14	135	17	13			11	111	10.1	7	0				2	D21, 22	51, 52	5016-5182
8/15	200	16	3	2	2	16	182	11.4	2	0					D22, 23	---	5191-5392
8/16	147	15	0	5	4	16	124	6.9	3	0					D23	50, 53	5400-5541
8/20	109	15	1	11	11	10	83	7.6	5	0					D23, 24	53, 54	5582-5682
8/21	154	16	8	2	2	9	101	11.22	13	8	2	22	5	4	D24, 25	54, 55	5693-5811
Total 33 Days	4822	480	96	125	107	403	4078	10.12	60	13	9	92	72	8	---	---	---

P = Polaroid
T = Tape

In addition, Table 5.1 contains:

11. Digital tape identification numbers.

12. Video tape identification numbers.

13. PPI photograph identification numbers recorded on 35 mm film.

Totals of all rain days in 1972 and 1973 appear on the last line for each year.

In an earlier discussion it was pointed out that digital tape equipment was not available at the start of the experiment. Thus, under 1972, no identification numbers appear for digital tapes. From 9 May to 24 May 1973 are listed DV identification numbers which mean digital tapes made from video tapes in "off-line" mode. Tape identification not bearing a D or DV refer to video tapes.

5.1.1 Radar Data Analysis (Volume II)

This report (Volume I) on the rain statistics experiment has dealt with various aspects of the experimental program and does not contain any significant discussion on data analysis. However, the analysis program was an important but parallel effort which had serious impact on the form of the experiment. Development of the concepts of the analysis program may be found in Ref. 5, 46, 47, 48 and 49.

In the course of performing the analysis, as is the case in most such programs, changes were made to the program as it progressed. Data reduction and analysis techniques and the statistical results as finally evolved can be found in Volume II of this report.

5.2 METEOROLOGICAL DATA

5.2.1 Sources of Data

The meteorological data have come from several sources:

a. Data generated by the Weather Service Office (WSO) at Wallops Station.

b. Teletype Service A (Flight Services) circuit 005 reports were provided by Wallops WSO.

c. Teletype Service C (Weather Service) circuit 31 reports were provided by Wallops WSO.

d. A teletype RAWARC circuit report was provided by Wallops WSO.

e. Facsimile Charts (National Schedule) were provided by Wallops WSO.

f. Fascimile Charts (Forecast Schedule) were obtained from the National Meteorological Center, Suitland, Maryland.

g. Fascimile Weather Radar maps transmitted by land lines from Patuxent River, Maryland were received at SPANDAR.

h. Radar weather forms prepared at Patuxent River, Maryland.

i. Data generated by APL personnel.

j. Hourly precipitation data for Maryland and Virginia locations issued monthly by the U.S. Department of Commerce, Asheville, North Carolina.

k. Climatological data for Maryland and Virginia locations, issued monthly by the U.S. Department of Commerce, Asheville, North Carolina.

l. Daily Weather Maps, Weekly Series, issued by the U.S. Department of Commerce and prepared at Suitland, Maryland.

m. Ocean Water Surface Temperature charts, issued monthly by the U.S. Coast Guard (Department of Transportation).

5.2.2 Data Catalog

Data have been extracted from the above sources and have been filed and are readily retrievable. The data are listed next; the source is identified parenthetically using identifiers in 5.2.1. (The numbers 5.2 in the listing of the above paragraph will be omitted for simplification.)

a. Wallops Island Rawinsonde evaluations of 0000Z and 1200Z soundings (1.a).

(1) Point values of height, pressure, temperature and dew-point depression reported at significant and mandatory levels.

(2) Showalter Stability index.

(3) Vertically averaged wind speed and direction reported at approximately 1000 ft intervals.

b. Wallops Island 0000Z rawinsonde evaluations at 1000 ft levels for periods of SPANDAR operations (1.a).

(1) Temperature, index of refraction, pressure, density, dew-point, relative humidity, absolute humidity, wind speed and direction.

c. Nearby rawinsonde data from stations within about 1000 km of Wallops Island (1.c). These contain same information as 2.a, above. Data for lower altitudes (under 50,000 ft) were filed.

d. Wallops Island Surface Observations form 10A (1.a). These give state of sky, weather, ceiling, visibility, sea level pressure, temperature, dew-point and surface wind speed and direction. These are given hourly from 1200Z to 2100Z, but on weekends are given at 1500Z, 1800Z, and 2100Z.

e. Wallops Island Surface Observations form 10B (1.a). This form supplements form 10A and gives time of beginning and ending of rain, showers, thunder, etc., and hourly amounts of precipitation.

f. Wallops Island rain gage charts (1.a). Weighing gage with time resolution about 3-4 min and rain resolution of .01 or .02 in.

g. Charts from rain gage located at Snow Hill VOR (1.i). Tipping bucket gage, each tip indicates 0.2 mm rain, with time resolution of about 0.1 to 0.2 min. Total rainfall measured separately.

h. Surface weather data from about 500 km radius (1.b). These are observations taken at airport stations. The data that were filed covered (1) periods when stations within 140 km of SPANDAR reported rain, and/or (2) periods when SPANDAR was taking data on rain. These data include observations of rain including intensity and thunder. There are also other meteorological surface observations of rain including intensity and thunder. There are also other meteorological surface observations in the airport reports.

i. Surface weather maps issued at 3-hour intervals (1.e). Daily surface weather maps (1.1).

j. Weather map analyses and summaries, particularly for rain periods (1.b and 1.c).

k. Upper Air Maps (1.e). These maps for the 850, 700, 500, 300, and 200 mb levels include wind, temperature, dew-point depression and heights and are issued twice daily. Also separate wind maps.

l. Weather Depiction charts (1.e.). These maps, issued eight times daily, show sky cover and ceiling.

m. Patuxent Radar facsimile charts (1.g). These transmissions were recorded three times per hour during the working day and show the PPI scope with annotations. There are also the radar weather forms (1.h).

n. Radar Depiction Charts (1.e). These charts, issued 14 times daily, give the combined analysis from the network of radar stations. Echo drift velocities are given; rain categorization and intensities are given.

o. Coded radar reports (1.b). These reports give the areas of returns with fractions of area covered, separate cells and their diameters. There is also an estimate of rain intensity, drift velocity and maximum heights. Echo intensities are given. The data retained were those that indicated rain in the SPANDAR area. Both Patuxent and Atlantic City radar reports are in the list of reporting stations.

p. Composite Moisture index chart (1.e). Issued twice daily, this contains four charts: a stability chart which contains both "lifted-index" and "K-index"; precipitable water (surface to 500 mb); freezing level (lowest level that $0^{\circ}C$ is reported if there is more than one level); and the average relative humidity (surface to 500 mb and weighted by pressure depth).

q. Relative Humidity/Vertical Velocity (1.e). Issued twice daily. The dynamically derived vertical velocities are the 700 mb (about 10,000 ft) values.

r. Lifted index chart (1.f).

s. Surface and 1000 to 500 mb thickness chart (1.e).

t. Vorticity charts (1.e). Both barotropic and baroclinic.

u. Three-dimensional trajectory forecasts (1.c). For selected cities. Also has K-index.

v. Climatological data (1.k). This includes the 24-hr precipitation as measured by cooperative observers as well as by the regular weather stations. There are about ten locations within 40 mi of SPANDAR and about double that within the SPANDAR observing range.

w. Hourly precipitation data (1.j). These contain reports from six stations with recording rain gages within the SPANDAR observing range.

x. Water temperatures (1.d and 1.m).

y. Miscellaneous Weather Service outputs (1.b,c,e,f). Synoptic discussions. Numerical products.

5.2.3 Data Reduction

Detailed tabulation and data reduction of the pertinent meteorological data are in Refs. 50, 51, 52, 53, and 54. These are considered as part of this Final Report and are included in Volume III as Appendix D.

5.2.4 1973 Rain Comparison

The total monthly rainfall in the summer of 1973 was compared with the 10-year period 1962-1971, Ref. 55. Table 5.2 gives for each of the summer months, the 10-year average, the 1973 average, the wettest and driest month and climatology based on an even longer period but using fewer stations.

Table 5.3 gives the average number of days of different rainfall amounts, based on the same 10-year period compared with that of 1973.

The tables show that the decision to have the 4 months of observation extend from May to August was a good one. The month of May

Table 5.2

Monthly Rainfall (in.)

	May	Jun	Jul	Aug	Sep
10-year average	2.7	3.4	3.8	4.1	3.3
1973 average	3.7	3.7	3.2	7.5	2.5
Average, wettest month	6.1 (1971)	5.6 (1963)	6.8 (1969)	8.7 (1967)	5.4 (1963)
Average, driest month	0.6 (1965)	1.2 (1971)	1.1 (1963)	1.1 (1966)	1.7 (1970)
Climatology	3.6	3.6	4.6	5.6	4.0

Table 5.3

Average Number of Days of Specified Rainfall

Rainfall Equals or Exceeds (in.)	May		Jun		Jul		Aug		Sep	
	Av	1973	Av	1973	Av	1973	Av	1973	Av	1973
.01	8.3	12.1	7.1	8.7	9.4	8.3	7.8	10.5	6.0	5.6
.1	5.4	8.7	5.3	5.1	6.4	5.5	5.5	8.2	4.3	3.4
.5	1.8	2.9	2.3	2.6	2.6	2.6	2.3	4.1	2.2	1.6
1.0	0.6	0.4	0.9	0.9	1.0	0.7	1.2	2.0	1.0	0.9

was rainier than the 10-year average and about the same as the longer period climatological value. There were substantially more days of measurable rain.

The month of June was about average with respect to amount of rain and number of rainy days. The month of July was drier than normal in amount of rain and somewhat below normal in terms of days of rain. August had substantially more rain and more days of rain. In total, the

summer observing months of 1973 had more rain than the 10-year average indicated and more days of rain, but it was no record-breaker. In terms of the total rainfall for the 10-year period and the 4 months of observation--a total of 40 months--1973 was wetter 60% of the time, drier 32% of the time and about the same (within 0.25 in. of rain) 8 % of the time.

6. ACKNOWLEDGMENTS

This experiment was a joint effort of NASA Goddard Space Flight Center (GSFC) and the Applied Physics Laboratory of The Johns Hopkins University (APL/JHU). The GSFC project manager was Dr. Jerome Eckerman. The principal investigators were Isadore Katz of APL/JHU and Dr. Robert K. Crane of MIT Lincoln Laboratory. Experiment manager for GSFC was Francis X. Downey and for APL/JHU was Thomas G. Konrad.

The Radar Atmospheric Research Facility (RARF) is a part of the NASA Wallops Island Station. Successful completion of this and other allied radar meteorology experiments are due in large measure to the continued support by R.L. Kreiger, Director, and many of his technical staff at Wallops Island.

Personnel of APL/JHU implemented the experiment. The various aspects of antenna measurements, calibration, frequency diversity, video tape recording, and mount control were carried out by W.L. Vann, R.C. Mallalieu, I.J. Sheppard, C.H. Ronnenburg, and H.H. Knapp. Operation and maintenance of the experimental equipment was carried out by J.C. Howard, N.R. Beasley, R.L. Gagnon, N.E. Gebo, L.D. Greer, H.L. Lord, C.W. Ponder, and H.K. Seemann. Direction of the operations was under A. Arnold, E.B. Dobson, J. Goldhirsh, R.A. Kropfli, and J.R. Rowland. Data reduction, processing and analysis were performed at APL/JHU and GSFC by J. Feraci, R.A. Kropfli, T.G. Konrad, M.W. Lawson, and J. Rosenberg. Typing of reports and manuscripts was done by L. Hofmann.

The radar controller and processor was designed, fabricated, and installed under M. Wall by E. Levine, W. Snyder and L. Wexler of Computer Sciences Corporation.

The support of NASA Headquarters is gratefully acknowledged through the offices of Dr. R.B. Marsten, Director of Communications Program and Jerome Freibaum, Program Manager of the Technical Consultative Services under which this experiment was funded.

Page intentionally left blank

7. REFERENCES

1. Crane, R.K., "Propagation Phenomena Affecting Satellite Communication Systems Operating in the Centimeter and Millimeter Wavelength Bands," Proc. IEEE 59, No. 2, February 1971, pp. 173-188.

2. Semplak, R.A. and Keller, H.E., "A Dense Network for Rapid Measurement of Rainfall Rate," Bell System Technical Journal, July-August 1969, pp. 1745-1756.

3. Katz, I., Konrad, T.G., Kropfli, R.A., "Satellite Communication Interference Caused by Scattering From Rain," Technical Proposal, 22 February 1971.

4. Katz, I., Konrad, T.G., Kropfli, R.A., "Equipment and Experimental Procedures for an Experiment on Statistics of Spatial Distribution of Rain," Technical Note No. 2, BPD71U-24, 26 August 1971.

5. Katz, I., Konrad, T.G., Kropfli, R.A., "Acquisition, Reduction and Analysis of Radar Rain Data," Technical Note No. 3, BPD71U-27, 13 October 1971.

6. Katz, I., Konrad, T.G., Kropfli, R.A., "Experiment on Statistics of the Spatial Distribution of Rain," Technical Note No. 4, BPD71U-28, 14 October 1971.

7. Katz, I., Konrad, T.G., Kropfli, R.A., "Alternate Approach," Draft of Technical Note, MPD72U-008, 1 February 1972.

8. Katz, I., Kropfli, R.A., Vann, W., "Response to Computer Sciences Corporation on Their Proposal to Modify the NASA Experiment Controller and Radar Video Processor," Technical Note No. 9, MPD72U-024, 15 June 1972.

9. Vann, W.L., "Status of Radar Modifications for the Rain Statistics Program to be Conducted at Wallops Island," Technical Note No. 8, MMS-947, 15 May 1972.

10. Katz, I., Konrad, T.G., Kropfli, R.A., Vann, W., "Description of 1972 Spatial Statistics of Rain Storms Experiment," Technical Note No. 11, MPD72U-036, 3 August 1972.

11. Konrad, T.G., "Experiment Plan for the 1973 CLC Program," MPD73U-020, 14 March 1973.

12. Kropfli, R.A., "Another Ultimate Radar for Weather Research," MPD73U-062, 29 August 1973.

13. Katz, I., "Operation Test Plan: May to September 1973," MPD73U-028, 13 April 1973.

14. Ronnenburg, C.H., Bassnett, A.J., Knapp, H.H., "A Frequency Diversity Source Developed for Rain Statistics Program," MED-SR/718, 20 June 1973.

15. Atlas, D., "Advances in Radar Meteorology," Advances in Geophysics, 10, Academic Press, N.Y., 1964, pp. 318-478.

16. Marshall, J.S. and Hitchfeld, W., "Interpretation of the Fluctuating Echo from Randomly Distributed Scatterers," Part 1, Can. J. Physics, 31, 1953, pp. 962-994.

17. Wallace, P.R., "Interpretation of the Fluctuating Echo from Randomly Distributed Scatterers," Part 2, Can. J. Physics, 31, 1953, pp. 995-1009.

18. Computer Sciences Corporation, Propagation Experiment Controller and Radar Video Processor, April 1972.

19. Kropfli, R.A., Konrad, T.G., "Further Specification of Software Requirements for the CSC Radar Controller and Video Processor," Technical Note No. 10, MPD72U-035, 24 July 1972.

20. Computer Sciences Corporation, "Technical Manual for Propagation Experiment Controller and Radar Video Processor," May 1973.

21. Computer Sciences Corporation, "Technical Manual for Propagation Experiment Controller and Radar Video Processor," January 1974.

22. Machamer, J.L., Becraft, W.A., Counihan, R.J. and Scaggs, S.L., "Video Tape Interface Unit," BID-T-1584, 20 September 1972.

23. "Update of Video Tape Interface Unit (VTIU) for Phase II (Summer 1973) Activities," BID-T-1683, 3 April 1973.

24. Konrad, T.G., "Program Plan for the Spatial Statistics of Rain Experiment," Technical Note No. 7, MPD72U-016, 10 May 1972.

25. Goldhirsh, J., "Statistical Calibration of SPANDAR," MPD72U-054, 29 November 1972.

26. Goldhirsh, J., "Sphere Calibration Program," MPD73U-011, 6 February 1973.

27. Vann, W.L., "Preliminary Results of the Rain Statistics Calibration Program on SPANDAR," MMS-1108, 21 February 1973.

28. Goldhirsh, J., Kropfli, R.A., "Inclusion of Atmosphere Attenuation Contribution in Radar Equation," MPD73U-014, 26 February 1973.

29. Vann, W.L., "SPANDAR Antenna Gain Measurement," MED-SR/697, 1 May 1973.

30. Goldhirsh, J., "Measured Radar Parameters and Error Budget Associated with SPANDAR and the CLC Program," MPD73U-054, 9 July 1973.

31. Vann, W.L., "Receiver Sensitivity Improvement to be Expected with SPANDAR Paramp," 12 September 1973.

32. Vann, W.L., "Final Report on SPANDAR Calibration Activities," MMS-1348, 12 September 1973.

33. Goldhirsh, J., Kropfli, R.A., "Addendum A to Operation Test Plan - Definitions of "Acceptable" and "Preferred" Regions," MPD73U-038, 3 May 1973.

34. Joss, J. and Waldvogel, A., "A Method to Improve the Accuracy of Radar-Measured Amounts of Precipitation," Fourteenth Radar Meteorology Conference, Tucson, Arizona, November 17, 1970, pp. 237-238.

35. Donaldson, R.J. and Tear, R.T., "Distortions in the Reflectivity Patterns by Antenna Side Lobes," Proc. 10th Radar Meteorology Conference, Boston, Massachusetts, AMS, 1963, pp. 108-115.

36. Austin, P.M. and Shaffner, M.R., "Computations and Experiments Relevant to Digital Processing of Weather Radar Echoes," Proc. 14th Radar Meteorological Conference, Boston, Mass., AMS, 1970, pp. 375-380.

37. Rogers, R.R., "The Effect of Variable Target Reflectivity on Weather Radar Measurements," Quart. Journal Roy. Met. Soc., 97, 1971, pp. 154-167.

38. Kropfli, R.A., "Multiple-Time Around Errors During the CLC Experiment," MPD73U-046, 14 May 1973.

39. Arnold, A., "Meteorological Information Desired for the Rain Study Preliminary," MPD72U-046, 25 October 1972.

40. Arnold, A., "Meteorological Aspects of Echo Field Characterization," MPD73U-019, 13 March 1973.

41. Arnold, A., "Request for Support from NASA/Wallops for Summer 1973 CLC Program," MPD73U-031, 19 April 1973

42. Arnold, A., "Meteorological Data Base, CLC Program," F1E73U-001, 20 October 1973.

43. Austin, P.M. and Houze, R.A., "Analysis of Mesoscale Precipitation Areas," 14th Radar Meteorology Conference, 1970, pp. 329-334.

44. Austin, P.M., "Some Statistics of the Small-Scale Distribution of Precipitation," Final Report, Contract NASA/ERC 0420, 1971.

45. Rice, P.L. and Holmberg, N.R., "Cumulative Time Statistics of Surface Rainfall Rates," ITS, 1971.

46. Kropfli, R.A., "Specifications and Logic for Reflectivity Contouring Program, MPD72U-015, 3 May 1972.

47. Goldhirsh, J., "Analysis Plan for CLC Experiments," MPD73U-025, 9 April 1973.

48. Kropfli, R.A., "Radar Data Reduction Plan for the CLC Experiment," MPD73U-036, 25 April 1973.

49. Lawson, M.W., "Description of the FORTRAN IV Program to Analyze High Resolution Radar Scans through Severe Thunderstorms," BCP-598, 25 October 1973.

50. Arnold, A., "Meteorological Summary for Periods of SPANDAR Rain Observations, May 1973," MPD73U-053, 29 June 1973.

51. Arnold, A., "Meteorological Summary for Periods of SPANDAR Rain Observations, June 1973," MPD73U-066, 10 September 1973.

52. Arnold, A., "Meteorological Summary for Periods of SPANDAR Observation During July 1973," MPD73U-070, 27 September 1973.

53. Arnold, A., "Meteorological Summary for Periods of SPANDAR Observations During August 1973," F1E73U-006, 3 December 1973.

54. Arnold, A., "Meteorological Data Analysis," MPD73U-027, 12 April 1973.

55. Arnold, A., "Comparison of 1973 Summer Rain Statistics With A Longer Period of Time," F1E74U-001, 5 January 1974.

56. Donaldson, R.J., "Improvement in Accuracy of Thunderstorm Echo Top Measurement," Proc. 11th Radar Meteorology Conference, Boston, Mass., AMS, 1964, pp. 288-291.

Page Intentionally Left Blank

8. CROSS-INDEX

Subject	Reference No.	Page
Waveguide Measurements	32	2
WSR 57	4	25
Z-R Mode	11	16

*U.S. GOVERNMENT PRINTING OFFICE: 1975 - 635-275/27

"The aeronautical and space activities of the United States shall be conducted so as to contribute . . . to the expansion of human knowledge of phenomena in the atmosphere and space. The Administration shall provide for the widest practicable and appropriate dissemination of information concerning its activities and the results thereof."

—NATIONAL AERONAUTICS AND SPACE ACT OF 1958

NASA SCIENTIFIC AND TECHNICAL PUBLICATIONS

TECHNICAL REPORTS: Scientific and technical information considered important, complete, and a lasting contribution to existing knowledge.

TECHNICAL NOTES: Information less broad in scope but nevertheless of importance as a contribution to existing knowledge.

TECHNICAL MEMORANDUMS: Information receiving limited distribution because of preliminary data, security classification, or other reasons. Also includes conference proceedings with either limited or unlimited distribution.

CONTRACTOR REPORTS: Scientific and technical information generated under a NASA contract or grant and considered an important contribution to existing knowledge.

TECHNICAL TRANSLATIONS: Information published in a foreign language considered to merit NASA distribution in English.

SPECIAL PUBLICATIONS: Information derived from or of value to NASA activities. Publications include final reports of major projects, monographs, data compilations, handbooks, sourcebooks, and special bibliographies.

TECHNOLOGY UTILIZATION PUBLICATIONS: Information on technology used by NASA that may be of particular interest in commercial and other non-aerospace applications. Publications include Tech Briefs, Technology Utilization Reports and Technology Surveys.

Details on the availability of these publications may be obtained from:

SCIENTIFIC AND TECHNICAL INFORMATION OFFICE

NATIONAL AERONAUTICS AND SPACE ADMINISTRATION

Washington, D.C. 20546